

Contents lists available at ScienceDirect

# Separation and Purification Technology

journal homepage: www.elsevier.com/locate/seppur



#### Review

# Adsorbent shaping as enabler for intensified pressure swing adsorption (PSA): A critical review

Dora-Andreea Chisăliță\*, Jurriaan Boon, Leonie Lücking

TNO Energy and Materials Transition, Sustainable Technologies for Industrial Processes, Westerduinweg 3, NL-1755LE Petten, the Netherlands

#### ARTICLE INFO

Editor: Z. Bao

Keywords: Pressure Swing Adsorption Adsorbent shaping Fast cycling Process intensification Machine learning

#### ABSTRACT

Pressure swing adsorption is widely applied in industry for hydrogen purification, methane recovery, air separation, biomass upgrading, CO2 recovery, to name a few. To further improve the attractiveness of pressure swing adsorption systems, ongoing research focusses on ways to intensify the process. In particular, improve productivity and reduce the footprint of the system consequently leading to reduced capital and operating costs. The proposed solution is known as fast or rapid cycling which, as the name implies, means to reduce the cycle time. However, there are some challenges to overcome such as mass transfer limitations leading to reduced separation efficiency, as well as increased pressure drop due to high superficial velocities typical to fast cycling. Adsorbent shaping has the potential to overcome these limitations and it is being regarded as a promising process intensification solution for pressure swing adsorption processes offering great flexibility in designing optimized cycles with improved performance. Various adsorbent shapes such as monoliths, laminates, foams and fibers have been studied in literature with monolith structures being the most popular. Most of the published literature on the topic of adsorbent shaping is concentrated on material development and lab-scale testing, modeling, and manufacturing through 3D printing techniques. Performance evaluations generally target reduced pressure drop and enhanced mass transfer kinetics with only a few papers addressing the broader context of process intensification and economic assessments of the potential gained benefits of using structured adsorbents in place of beads or pellets. Although, sorbent shaping is a very promising developing field, there is still significant work to be done for it to reach its full potential. Further research should go beyond shape optimization and lab-scale testing to process optimization and pilot/large-scale testing under cyclic conditions. In this context, newly developed artificial intelligence tools show great promise for the development of intensified cycles based on structured adsorbents by speeding up computation time of complex optimization routines. To date, there are limited industrial applications using structures sorbents. One of the main hurdles for large scale deployments is the labor and time intensive preparation methods currently available, leading to high manufacturing costs. Thus, development of easy, fast and cost-effective manufacturing options through automatization, will expedite the large-scale implementation of structured adsorbents in pressure swing adsorption processes.

# 1. Introduction

The term "adsorption process" refers to a unit operation in which a substance is separated from a fluid by affinity with a solid substrate, the adsorbent. Periodic regeneration of the loaded adsorbent in a two or

more column unit allows for a continuous process. Pressure swing adsorption (PSA) refers to a system using a change in pressure for the regeneration of the adsorbent. Potentially, a purge gas is used to further facilitate the regeneration. Developed since the 1970s, typical industrial applications of pressure swing adsorption include hydrogen purification, methane recovery, and air separation [1]. More recently, in the

Abbreviations: AE, Algebraic Equations; ANN, Artificial Neural Network; CFD, Computational Fluid Dynamics; COF, Covalent Organic Framework; cpsi, cells per square inch; DAC, Direct Air Capture; DAE, Differential — Algebraic Equations; DNN, Deep Neural Networks; L/D, Length over diameter ratio; LDF, Linear Driving Force; MOF, Metal Organic Framework; MTZ, Mass Transfer Zone; PDAE, Partial Differential and Algebraic Equations; PSA, Pressure Swing Adsorption; RCPSA, Rapid Cycle Pressure Swing Adsorption; RCPSA, Rapid Cycle Pressure Swing Adsorption; VPSA, Vacuum Pressure Swing Adsorption; WC, Working Capacity; ZIF, Zeolitic Imidazolate Framework; PINN, Physics-Informed Neural Networks.

E-mail address: dora.chisalita@tno.nl (D.-A. Chisăliță).

https://doi.org/10.1016/j.seppur.2024.128466

Received 26 February 2024; Received in revised form 10 June 2024; Accepted 15 June 2024 Available online 16 June 2024

1383-5866/© 2024 The Authors. Published by Elsevier B.V. This is an open access article under the CC BY-NC-ND license (http://creativecommons.org/licenses/by-nc-nd/4.0/).

<sup>\*</sup> Corresponding author.

List of symbols		$rac{ m r_{iD}}{ m r_o}$	fiber inner radius [m] outer radius [m]	
a	inside diameter hollow cylinder [m]	r <sub>oD</sub>	fiber outer radius [m]	
$A_{\rm p}$	particle surface area [m <sup>2</sup> ]	r <sub>p</sub>	particle radius [m]	
b	outside diameter hollow cylinder [m]	$u_0$	superficial fluid velocity [m/s]	
$C_{D}$	cell density [cpsi]	$u_g$	interstitial gas velocity [m/s]	
ď	diameter of a sphere of equal volume/surface area ratio as	$V_{ m fib}$	bed volume fraction occupied by fibers	
	the particle [m]	$V_{p}$	particle volume [m <sup>3</sup> ]	
ď″	diameter of equivalent volume sphere [m]		•	
D <sub>e</sub>	effective pore diffusivity [m <sup>2</sup> /s]		teristic numbers	
$d_{f,out}$	fiber outer diameter [m]	Bi	Biot number [–]	
$d_h$	channel hydraulic diameter [m]	Nu	Nusselt number [–]	
D <sub>m</sub>	molecular diffusivity [m²/s]	Pé	Péclet number [–]	
	particle diameter [m]	Pr	Prandtl number [–]	
$d_p$	•	Re	Reynolds number [–]	
$d_{p,eq}$	equivalent sphere diameter [m]	Sc	Schmit number [–]	
d <sub>t</sub>	column diameter [m]	Sh	Sherwood number [-]	
$D_{Z}$	axial dispersion [m²/s]			
f	correction factor [–]	Greek l	letters	
f'	friction factor	$\delta_a$	adsorbent coating thickness [m]	
k <sub>e</sub>	material thermal conductivity [W/m²K]	$\delta_{\rm w}$	wall thickness [m]	
kg	gas thermal conductivity [W/m <sup>2</sup> K]	ε	bed voidage [–]	
$k_{ m LDF}$	linear driving force mass transfer coefficient [1/s]	$\varepsilon_{ m hc}$	void fraction of bed of hollow cylinders [-]	
1	channel side length [m]	$\varepsilon_{\rm sc}$	void fraction of bed of hollow cylinder corrected to soli	
L	column length [m]	- 30	cylinders [–]	
q	average amount adsorbed [mol/kg]	μ	dynamic viscosity [Pa*s]	
q*	amount adsorbed at equilibrium [mol/kg]	ρ	fluid density [kg/m <sup>3</sup> ]	
$r_{fs}$	radius of Happel's free surface [m]: $r_{fs} = \frac{r_{oD}}{\sqrt{V_{co}}}$	ф	sphericity [–]	
r <sub>i</sub>	inner radius [m]	Ψ	spheretty [-]	

industrial energy transition, novel processes are being developed utilizing PSA systems for the recovery of CO<sub>2</sub> [2] and carbon monoxide [3], and the upgrading of biogas [4]. More advanced PSA applications include sorption-enhanced reactions for the enhancement of reactions through the use of an in situ adsorbent material [5–9].

In order to further improve the attractiveness of PSA, continuous efforts are being made to intensify the process. Process intensification reduces the footprint of the system and positively impacts capital and operating costs. The footprint can be reduced by fast cycling as the size of columns is determined also by the cycle time. Faster adsorption and regeneration of the adsorbent material means less material is needed and consequently smaller columns are possible. The performance of adsorption-based gas separation processes is dependent on the design of the process, the choice of material as well as its shape. Adsorption processes are generally carried out in packed bed columns with the adsorbing material in the form of beads or pellets. This type of material shaping has the benefit of high adsorption loading, easy and fast manufacturing, and thus low costs. However they suffer from serious drawbacks in terms of process efficiency due to high pressure drop and limiting mass and heat transport phenomena [10,11]. In conventional packed bed systems, the pressure drop has a direct influence on the energy consumption, product recovery and purity as well as on the productivity. One way to prevent high pressure drops is to adopt radial bed adsorbers however, this leads to increased complexity and costs [12]. Mass and heat transfer limitation may occur due to long diffusion paths through the material pores leading to reduced performance [10]. In particular during fast cycling, where these intra-particle mass and heat transfer limitations become the main limitation of the performance which may cause unwanted breakthrough of the gas [12]. An option for mitigating mass transfer limitations would be to reduce the size of the bed packing. In the last decades, particle sizes were reduced from 3 mm to 0.7 mm, reducing not just the diameter of the packing material but also the lengths over diameter ratios (L/D) to < 1 resulting in "pancake" geometries in order to reduce pressure drop. This leads to the rise of other complications such as gas maldistribution and even fluidization of the packed bed [12]. Geometric structuring has the potential of overcoming these limitations and improve the performance of the process due to increased void fractions and surface area allowing for high superficial velocities favored in rapid cycling leading to reduction in column size with no negative consequences on the pressure drop [11,13,14]. On the other hand, when employing structured adsorbents the productivity might suffer due to reduced adsorbent loading compared to their traditional counterparts. Nonetheless, due to reduced pressure drop, structured adsorbents are able to process 15–30 times higher flowrates which is generally enough to compensate for the lower adsorbent loading [15].

This review critically discusses the available literature on structured adsorbents, an important emerging topic which has not been discussed in a dedicated review to date. Papers have been published in the last decade that review the application of MOF-based adsorbents [16–18], zeolite-based separations [19,20], separation of rare earth elements [21], electric-swing adsorption [22], and separation of carbon dioxide [23-25]. The topic of material shaping in the field of heterogeneous catalysis has also been thoroughly reviewed [26-30], and will not be discussed here. Hierarchically structured porous material is another type of shaping focused on the internal structure of the material. It shows high performance in various application areas like energy, catalysis, separation, adsorption, and biomedicine. The topic has been extensively reviewed including characterisation [31], synthesis [32,33], applications [34,35] and will not be further discussed. Hierarchically structured porous materials can also be further shaped into different geometries for enhanced performance [36]. Finally, additive manufacturing techniques for catalysts and adsorbents have shown great progress over the last decade and were recently reviewed by Rosseau et al. [37]. Consequently, additive manufacturing and 3D printing techniques will be discussed below, only to the extent that they enable advances in process intensification of pressure swing adsorption.

With the focus on the intensification of adsorption-based separation

processes, this review first discusses sorbent manufacturing techniques, followed by a summary of literature discussing the potential of sorbent shaping. The advanced sorbent shapes enable the design of improved, intensified pressure swing adsorption cycles. Novel optimisations need to be done in order to maximise the potential for intensification: reassessing the trade-offs between bed density and pressure drop, sorbent density and resistances to heat and mass transfer, enabling faster cycling and higher throughputs. These are enabled by advanced cycle modelling of processes using structured adsorbents, which is discussed in a separate section, and is followed by an outlook and discussion of promising research directions.

# 2. Manufacturing of structured adsorbents

Converting powder material into desired shapes is not straightforward. Material properties such as adsorption capacity and porosity, as well as mechanical strength should be maintained as much as possible. An overview of the most applied shaping methods is presented in Table 1. Conventional shapes such as pellets, beads and extrudates are obtained by one of the variety of traditional manufacturing approaches like pelletizing, spray drying and granulation, casting, or extrusion. Amongst these techniques, extrusion is capable of manufacturing more complex shapes like hollow cylinders, or monoliths with continuous channel design. From a shaping perspective, recently developed adsorbents, including MOF and COF, not only provide enhanced equilibrium and intrinsic kinetics – they also provide ample opportunity for shaping. COFs more than MOFs have been demonstrated with very high thermal conductivities [38,39]. However, some materials such as those containing organic compounds (e.g., MOFs, COFs) are not suitable to be shaped using these methods due to the destructive nature of the thermal treatment on the porous structure as well as the low mechanical strength they possess which excludes any manufacturing process that applies pressure [40]. The use of pressure to shape the powder can also lead to reduced porosity or pore blockage having a negative influence on the adsorption properties. Furthermore, some of these manufacturing methods (e.g., casting, coating) require an additional support material to attain stable structures which may lead to reduced adsorption loading of the structured adsorbent [41]. 3D printing, known also as additive manufacturing, has been promoted in the last decade as the option to shape porous adsorbents into complex structures. There are seven categories of additive manufacturing technologies available so far, with new methods and technologies being constantly developed: 1) binder jetting, 2) direct energy deposition, 3) material extrusion, 4) material jetting, 5) powder bed fusion, 6) sheet lamination, and 7) vat polymerization. Each of these technologies include different techniques under their umbrella. For adsorbent manufacturing the main applied technologies so far are vat polymerization and material extrusion [41]. Reviews on the different 3D printing techniques, their advantages and disadvantage, the status of developments and applications, were recently published by several authors [37,40-42]. Although additive manufacturing techniques offer great flexibility in terms of shapes and material loading, the major hurdle for large scale deployment is the long preparation time [43]. Amongst the barriers that need to be overcome for scale-up is the standardization of the ink preparation which currently is technology and material dependent and still requires a lot of manual tuning making it labor and time intensive, and thus expensive. Stereolithography (SLA) and Digital Light Processing (DPL) have been identified as promising technics to overcome this issues as they are capable of simultaneously printing multiple geometries on the same printer, they are suitable for a wide range of materials and show improved printing accuracy [44,45]. They fell under the VAT polymerization techniques and use UV light to solidify the mixture of photosensitive resin and active material. SLA is not a new technology, it has been around since the early 1980s and has become more popular with the development of low-cost resins. With further advancements in process control, automatization of the manufacturing process could reduce the effort and printing time of other 3D printing technologies and improve accuracy, speeding-up industrial deployment. As the application of 3D printing techniques is expanding also into other areas of application (e.g., catalysis, electronics, drug delivery, thermal management, food), it is expected that the maturity of the shaping technology will grow and the associated costs will most likely drop.

Successful large-scale implementation of any 3D printed technique will also rely on process intensification, advancing additional features to set it further apart from conventional shaping techniques, such as binder-less printing, introduction of local structural variations and multi-material printing. Binder-less printing, even though possible from a material perspective, it is still a challenge due to rheological and light transmittance properties of the adsorbent material required for the 3D printing process. To this end, additives are introduced which in some cases can be removed by post-processing techniques, such as heat. But his could lead to other issues such as shrinkage of the structure postprocessing. In particular for materials based on organic compounds, preparing binder-free structures is still challenging, with only a few papers reporting novel manufacturing binder-free techniques based on controlling the evaporation of the solvent [46], or by using aqueous colloidal ink formulation [47]. Additional research is still required to find new ways to modify the raw material in such a way that it can meet printing requirements without significantly affecting its adoption properties.

As highlighted by Rosseau et al. [37], most of the existing literature on 3D printing focuses primarily on the chemistry of ink formulation, printing optimization and small-scale testing of the printed structures, with little regard to shape optimization for the various large-scale applications. Amongst the strategies proposed for scale-up are stacking of multiple structures, or the use of multiple reactors similarly to a multitubular reactor. Both strategies have their advantages and disadvantages. In case of stacking multiple structures on top of each other, existing columns can be easily used but care must be taken to align the channels when loading the structures into the column. Similarly with multitubular reactors used in industry, when considering using multiple smaller reactors as a scale-up strategy, one of the challenges is maintaining even distribution of flow across the multiple reactors even though the pressure drop will stay the same over the different tubes as a result of identical structures. This concept may also lead to somewhat increased cost with scale-up as the economy of scale does not completely apply. Reactor scale-up is closely dependent on the developments in 3D printing, in particular ink formulations that can provide mechanically stable structures with minimal or no binder use. Most of the available literature reports cm-scale structures mainly due to the proof-ofprinciple type of research. In a recent study, Krishnamurthy et al. [48] studied the feasibility of scaling-up a 3D printed sorbent from laboratory scale to production scale, that is in the scale of 100 s kgs. Monolith structures were prepared from 8 kg of paste having a diameter of 50 mm and a height of 200 mm. For the scale-up evaluation, 90 such monoliths of 13X-AC were printed over a total manufacturing time of 4 weeks, corresponding to seven 1.75 m columns of stacked structures, clustered in 133 trains for the capture of 14,000 kg mol/hr of CO2, representing the flue gas of an 800 MW powerplant. The structures were characterized and tested in the lab along with simulations and technoeconomic assessment showing a 5 % reduction in the levelized cost of electricity and ~11 % reduction in footprint for the monolith case compared to the reference packed-bed using pellets. The results of this study clearly show there is strong potential in cost and footprint reduction by adopting structured adsorbents.

# 3. Adsorption processes using structured adsorbents

Structured materials are already extensively applied in the chemical industry for a variety of applications like air dehumidification or separation, vehicle exhaust treatment, hydrogen separation, CO<sub>2</sub> separation. A rapid cycle pressure swing adsorption (RCPSA) process developed

**Table 1** Overview of shaping methods.

Manufacturing approach	Shape obtained	Principle	Advantages	Limitations
Granulation	Granules / beads	Material is mixed with a binding agent and fed into a granulator apparatus	Straightforward, inexpensive	Low geometric flexibility; nor homogeneous shapes;
Spray drying	Granules / beads	Shape formed by atomizing a slurry containing the powder material followed by drying with hot gas/air	Good control over:  - particle size and distribution,  - residual moisture content,  - bulk density and - morphology. Straightforward and inexpensive High material versatility	Low geometric flexibility
Pelletizing / dry pressing	Pellets, tablets	Material powder is compressed in to form pellets or tablets	Fast preparation time High material versatility	Low geometric flexibility;
Spinning	Fibers	The solution containing the active material goes through a phase inversion process solidifying along a certain trajectory	Inexpensive and scalable technique Flexibility in adjusting adsorption properties	Low geometric flexibility;
Casting	Foams, monoliths	Colloidal suspension casted onto a mold	Able to produce complex shapes	Reduced material loading
Pulsed current processing (PCP)	Monoliths	Material powder packed in a die and introduced to a pulsed electric current followed by a thermal treatment	Binder-free; Minor loss of surface area; Mechanically stable; Applicable to micro- meso- and macro-porous powders	Requires identification of temperature and pressure ranges to achieve required porosity
Coating	Monoliths, fibers, laminates, foams	Material deposited on the surface of a support of the desired shape	Good control over active layer thickness; High material versatility	Low active material loading; some techniques are time consuming
Extrusion	pellets, monoliths	The powder material is mixed with different binders and additives and formed into the desired shape by applying pressure followed by a thermal treatment.	The most widely used method; Able to produce more complex structures (e.g., honeycomb, hollow cylinders).	The paste created must possess appropriate rheological properties; Requires the addition of permanent binders; Monoliths' wall thickness and cell density can be varied in a limited range
Additive manufacturing (3D printing)	Various shapes	An ink is prepared similarly to that used in extrusion. The structure is build layer by layer forming the desired design	Minimal material waste; High material flexibility; Easy optimization of the structure properties	Early stages of development

jointly by ExxonMobil Research and Engineering and QuestAir Technologies Inc., marketed under the name "QuestAir H-6200", is used for hydrogen recovery in hydrocarbon processing industries [49]. A significant increase in productivity is reported compared to a system operating with beads, as a result of up to 100 times higher mass transfer coefficients. For CO2 capture applications there are a few commercial technologies known to employ structured adsorbents. Direct air capture (DAC) modules use solid adsorbents in the shape of monoliths or filter sheet by companies like Global Thermostat [50] and Climeworks [51]. Another example is VeloxoTherm<sup>TM</sup>, developed by Svante Technologies Inc. The process, illustrated in Fig. 1, uses structured MOF laminate beds in a rapid cycle-temperature swing adsorption (RCTSA) [52,53]. Reported benefits of the structured adsorbent bed include a reduction in pressure drop by one to two orders of magnitude compared to conventional packed bed systems, up to 4 times increase in surface area compared to granular adsorbents, improved mass and heat transfer as well as faster kinetics thanks to shorter diffusion paths, smaller equipment and as a result reduced equipment cost [54]. Structured packed beds are also used to improve contact between two phases in process like absorption, stripping or distillation [55].

Various adsorbent shapes as illustrated in Fig. 2, have been studied in literature with monoliths being the most popular ones. The performance, and consequently the application of monolith structures depends on various geometric properties such as channel size and shape, wall thickness and cell density. A comparative study on the performance of a gas separation process using the sorbent material in the form of beads and as a structured monolith was conducted by Mosca et al. [10]. It was found that the use of structured adsorbent resulted in a reduction of 45 times in pressure drop while maintaining the same adsorption capacity as the beads. Beads and monolith structures were also evaluated by Middelkoop et al. [56] and found that beads showed a higher adsorption capacity but the adsorption/desorption rates were significantly faster for monoliths.

Zeolite monoliths with hierarchical pore structure were prepared and tested against pellets by Hasan et al. [57]. Enhanced mass transfer



Fig. 1. VeloxoTherm™ compact Rotary Adsorption Machine (RAM) of Svante using structured solid sorbent. Reprinted with permission from Ghaffari-Nik et al. (2022) [53].



**Fig. 2.** Illustration of a variety of adsorbent structures including (left to right): ceramic and carbon adsorbent monoliths, corrugated paper monoliths (center), fabric adsorbent and conventional beaded adsorbents. Reprinted with permission from Rezaei and Webley (2010) [12].

with a six times increase in effective diffusivity was observed for the monolith structure, as well as reduced pressure drop at similar adsorption capacity showing good potential for RPSA applications. Sharma et al. [13] evaluated the performance of a monolithic adsorbent against a packed bed of pellets in a vacuum pressure swing adsorption (VPSA) system considering equal volume columns. The results showed that the pelleted adsorbent system could not reach the same recovery rate unless higher vacuum is applied increasing the energy penalty of the process. The proposed monolithic VPSA process was also compared with a conventional amine-based CO<sub>2</sub> capture system showing improved performance in terms of productivity and exergy input. Krishnamurthy [58] carried out optimization of various cycle designs of a 6-step VPSA process for CO2 capture that lead to a two-folds increase in productivity (reported based on adsorbent volume) in case of 3D printed monolith sorbent structure, as well as a reduction in specific energy compared to a packed bed of pellets as shown in Fig. 3. This work was carried out as part of the ACT 3D-CAPS project part of which the design, 3D printing and testing of adsorbents for CO2 capture was previously investigated Γ14.591.

Tegeler et al. [60] showed that by changing the channel types in a monolith structure from straight to helical, the mass transfer rate was significantly improved leading to overall cost reduction of 30 % for a DAC system. In their approach, the helical shape of the adsorbent introduced convective transport of adsorbate towards the adsorbent wall (Fig. 4), which resulted in a significant enhancement of mass transfer rates.

Henrique et al. (2023) [36] have studied hollow structured monoliths made out of active carbon, with 8 tetragonal cubic centered unit cells each unit cell having a diameter of 5.7 mm and a thread diameter of 2 mm (Fig. 5) for the separation of C5-C6 alkane isomers. Breakthrough experiments were carried out to assess the adsorption of C5-C6 alkane isomers and evaluate the separation performance. Two different separation mechanisms were observed depending if the structure underwent an activation process or not. In case of the nonactivated structure it was shown that molecular sieving properties can be achieved also by materials with nonuniform pore size distribution. Different activation conditions (time, temperature) were evaluated leading to variations in the porosity of the structures by introducing additional micropores without greatly influencing the mesoporosity. After activation, alkanes were adsorbed in order of their boiling points following a thermodynamic mechanism instead. An increase in sorption capacity as well as in mixture loading was observed for the activated structures successfully

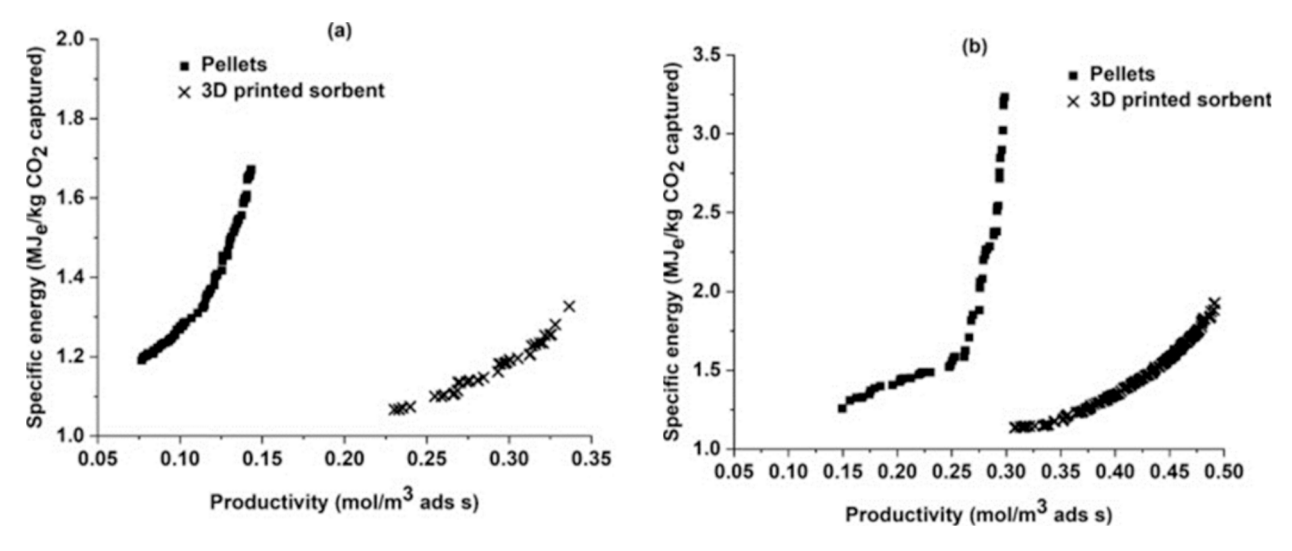
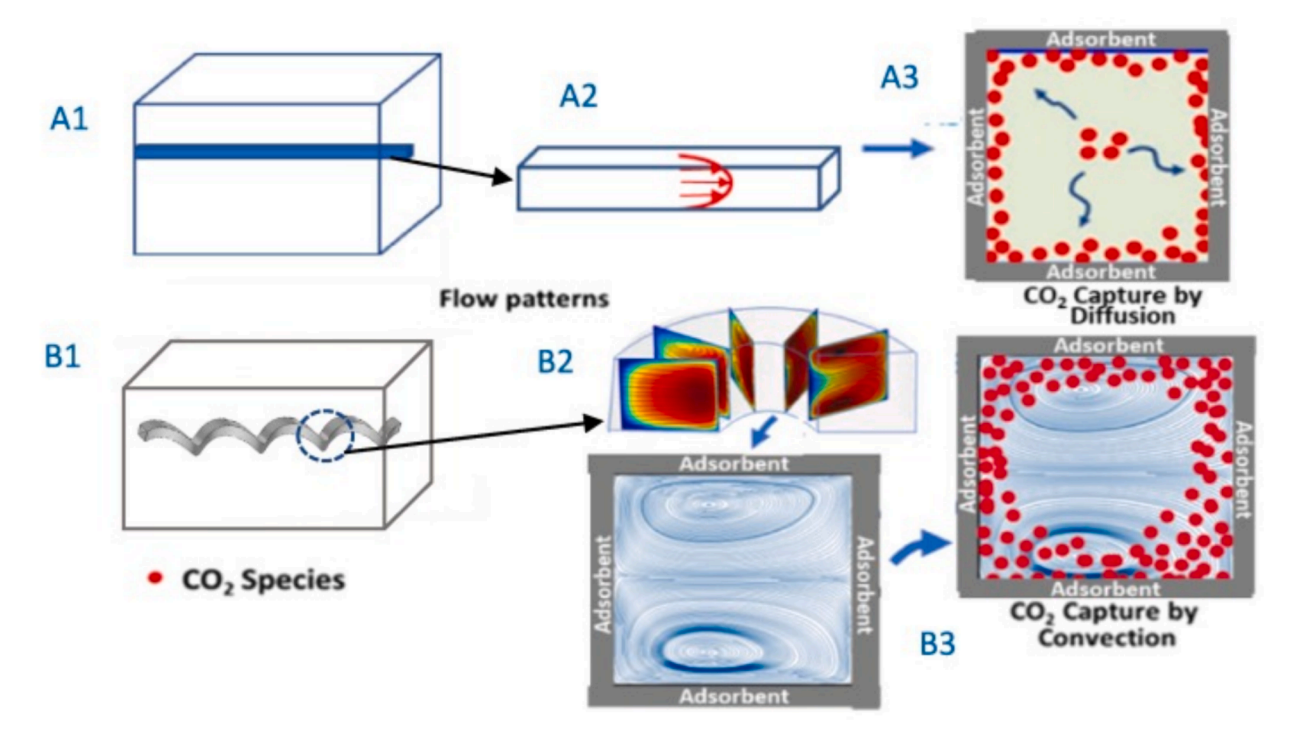


Fig. 3. Post-combustion carbon capture with VPSA: specific energy vs productivity pareto 3D printed silica sorbent grafted with amino silane and reference pellets for a lower bound of (a) 0.1 bar and (b) 0.01 bar. Reprinted with permission from Krishnamurthy (2022) [58].



**Fig. 4.** Figure demonstrating the benefit of a helical channel over a conventional honeycomb contactor. A1: Contactor with straight channels (a single channel shown for discussion purposes). A2: Laminar flow in straight channels. A3: CO<sub>2</sub> capture through diffusion. B1: Helical channels, B2: formation of Dean vortices. B3: Faster CO<sub>2</sub> capture rate via convection. Reprinted with permission from Tegeler et al. (2023) [60].

proving the applicability of structured sorbents in the field of alkanes separation.

Jeong and Realff (2021) [61] showed that monolith-shaped adsorbents enable the realization of modularized reactors with increased flexibility to adapt to various feeding conditions (e.g., input  $\rm CO_2$  concentration, cycle time, flow rate) (Fig. 6). They observed that reduction of cycle time is crucial in reducing cost. The proposed modularized reactor is also capable of changing the configuration of the adsorption/desorption steps during the process leading to better separation performance than a conventional fixed bed reactor.

Besides monoliths, other structures such as laminate and foam were also assessed against their pellet counterpart. Laminates can be considered as simplified monoliths but with a more complex manufacturing process. The evaluation of laminate adsorbent structures is comparatively reported less with only a handful of patents available [62–65] while foams have been previously studied as catalyst structures [66–70]. Rezaei and Webley [71] developed an analytical framework for finding the optimum set of geometric parameters (i.e., voidage, surface area per unit volume, bulk density) a structure should possess to lead to the best performance in terms of pressure drop, mass transfer zone, productivity. The most promising results for laminate systems were observed in case of small spacings and sheet widths of 0.2 mm. Similarly, He et al. [72] found that mass transfer resistance decreased and sharper breakthrough curves were observed with a reduction of the interlaminar spacing. The performance of monolithic structures depends not only on high cell densities (>1000 cpsi) and low voidages, but it is

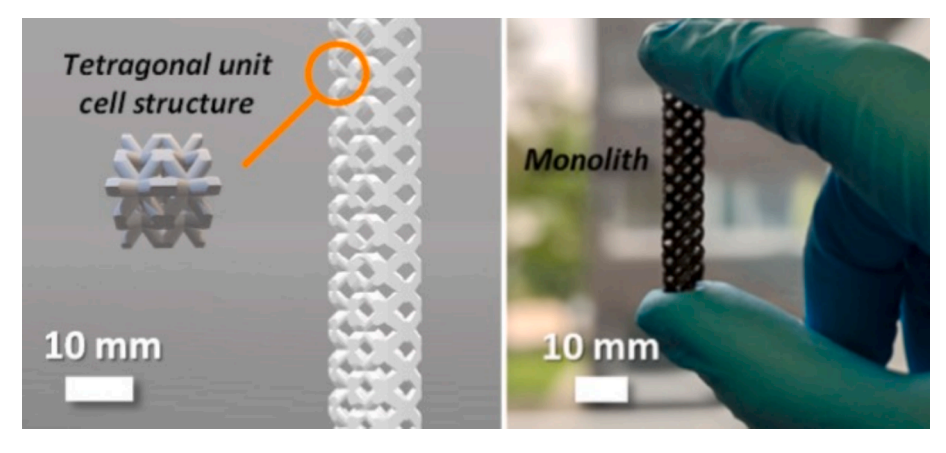


Fig. 5. Active carbon 3D printed monoliths for C5-C6 isomer separation. Reprinted with permission from Henrique et al. (2023) [36].

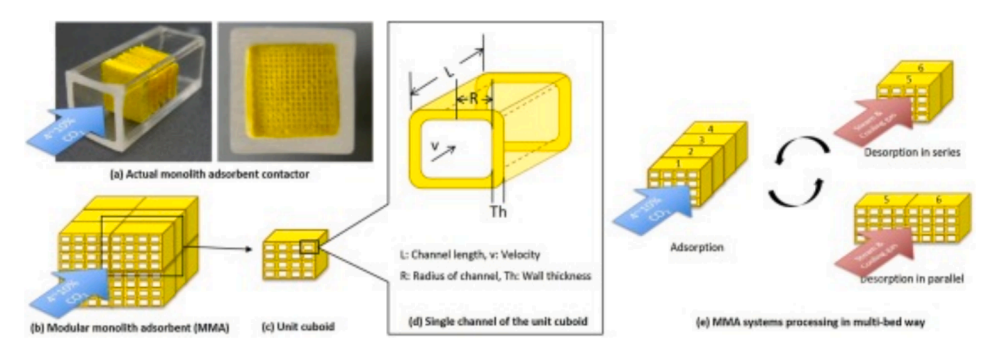


Fig. 6. Modular monolith adsorbents allow different configurations and cycle design including true moving bed configurations: (a) actual modular monolith systems for experiments, (b) conceptual design of the modular monolith systems, (c) unit block having specific dimensions, (d) dimensions of a single channel for the mathematical model, (e) true moving bed in modular monolith systems. Reprinted with permission from Jeong & Realff (2021) [61].

also highly dependent on the effective diffusivities that can be obtained in the walls of the monolith. High density monoliths with high surface areas are desired in order to outperform packed beds. The influence of geometric properties such as cell density and porosity was evaluated in terms of adsorption capacity and kinetics for 3D reprinted zeolite monoliths by Lawson et al. [73]. Contrarily to Rezaei and Webley [71], the authors found that low density monoliths (e.g., 200 cpsi vs 600 cpsi) together with enhanced microporosity performed better in dynamic operation as a result of reduced diffusional resistances. In case of high density monoliths (e.g., 600 cpsi) the best separation was obtained at low inlet velocities which would require long cycle times and could lead to poor recovery, thus not being industrially feasible. In case of foam structures, the study of Rezaei and Webley [71] showed comparable properties to packed beds of 0.7 mm diameter beads. The influence of the axial dispersion to the overall rate constant was found to be negligible for all evaluated structures. On the other hand, the internal rate and the external film contributions were found to have a more significant contribution. Another important finding by Rezaei and Webley [71] is that higher productivities can be achieved by using structured adsorbents with the condition that the system is operated at its optimal velocity in order to reduce pressure drop and mass transfer zone. Similar conclusion was noted by Sharma et al. [13] who compared monoliths with pellets in a VPSA process. Adsorbent-coated microchannel monolith was evaluated for natural gas purification in a PSA system by Pahinkar et al. [74]. From the parametric study it was observed that adjusting the channel size had a positive effect on depressurization efficiency and overall on reducing the total cycle time and consequently the plant size compared to conventional PSA processes.

Another type of structure that is gaining a lot of interest is fiber adsorbents. They were first applied for adsorption processes about three decades ago using a shell-and tube configuration with adsorbent

material present either in the bore or the shell of the fiber [75]. Feng et al. [76] investigated experimentally the performance of hollow adsorbents with adsorbent in the shell side for hydrogen separation in a PSA systems. A large gas separation efficiency was found as a result of reduced pressure drop and fast mass transfer rates.

More recently, fiber adsorbents with a hollow bore in which a heat transfer fluid can help efficiently control the temperature during adsorption-desorption cycles was found of particular interest for temperature swing adsorption (TSA) applications [78,79]. On the other hand, for applications where isothermal conditions can be expected, the fiber adsorbents can be produced in a monolith-type of structure without bore as illustrated in Fig. 7. Sujan et al. [77] prepared such a fiber sorbent and measured breakthrough curves for N2 and O2 at conditions typical to an air separation PSA system. A VPSA system for the kinetic separation of propane-propylene feed using a ZIF-8-based fiber sorbents (Fig. 8) is reported for the first time by Pimentel and Lively [80]. With a unoptimized cycle they were able to obtain up to 81 % propane purity and about 30 % recovery from an equimolar feed mixture. Further research is required to improve recovery rate while not significantly reducing the purity and reach competitive performance with the state-of the-art.

An economic evaluation of a small scale hydrogen purification PSA system using a zeolite-based hollow-fiber absorbent was performed by Ohs et al. [81]. Following optimization of hollow fiber design, operating pressure and adsorption time, a 13 % cost reduction was obtained compared to a reference case based on previously reported works [82–85]. Optimal fiber geometry was found to be weakly dependent on the adsorption capacity, with high product purities achievable by using modularized systems. A comparison between packed bed of pellets and hollow fiber structure for propylene-propane separation by VPSA was performed by Sen et al. [86]. From the parametric comparison it was

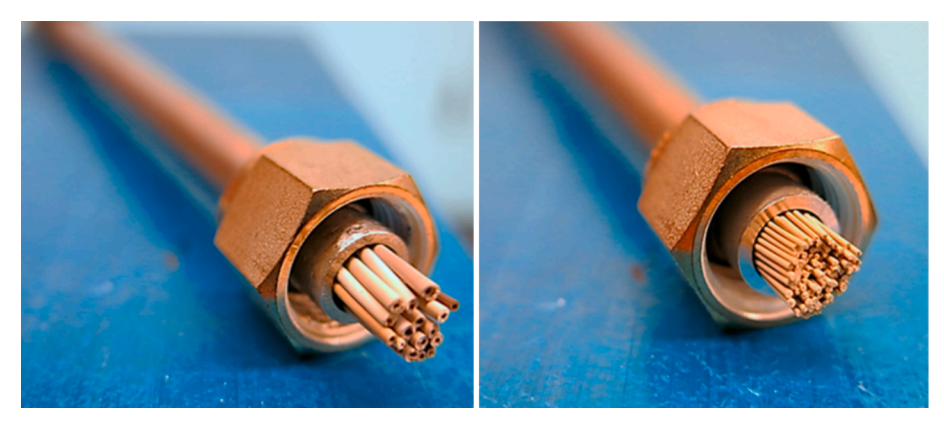
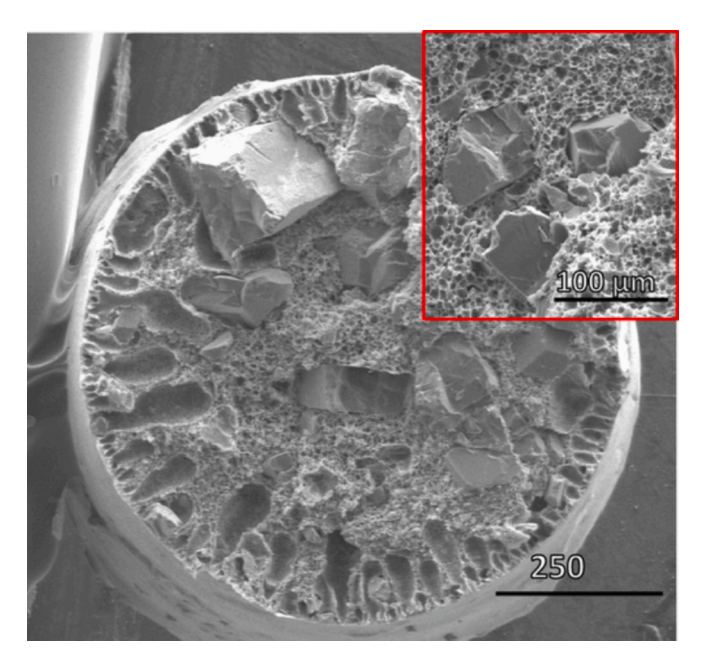


Fig. 7. Stainless steel hollow fiber module (left) and monolithic fiber module (right). Reprinted with permission from Sujan et al. (2018) [77].



**Fig. 8.** Fiber-shaped ZIF-8 adsorbents, with large crystals dispersed throughout the polymer matrix. Reprinted with permission from Pimentel & Lively (2018) [80].

observed that the hollow fiber adsorbent led to better performance regarding pressure drop, mass and heat transfer. As a result, a five times higher productivity (based on adsorbent weight) was calculated for the structured bed, considering the same volumetric flowrate and pressure drop as well as identical product purity and recovery rates in both systems. A critical review of fiber adsorbent based on microporous active materials has been published by Lee et al. [87] discussing the current status and future potential of these type of structured adsorbents in separation processes.

From work done in the field of catalysis, more simple shapes, that can be easily manufactured by currently available extrusion techniques, show benefits in term of reduced pressure drop and enhanced transfer phenomena compared to classical shapes like beads and pellets. Shapes like hollow cylinders or spheres, multilobed particles can also be applied for sorption applications. Compared to catalysts, shapes used for adsorption applications should be made predominantly from the adsorbent material in order to maintain satisfactory sorption capacities. Pashchenko [88] evaluated both experimentally and computationally the pressure drop inside a packed bed filled with various catalyst shapes such as full cylinders, hollow cylinders (i.e., raschig ring), convex cylinder with seven internal holes and speres with seven internal holes. A

linear dependence was reported between the pressure drop and the length of the packed bed while the velocity follows a quadratic dependance for all evaluated shapes. As seen from Fig. 9 the lowest pressure drop was observed for the bed of speres with seven internal holes followed by convex cylinders with seven internal holes, hollow cylinders and finally the full cylinders at velocities between 0.2-1.4 m/s in a bed with a length of 600 mm and a diameter of 100 mm. Gopal Manoharan and Buwa [89] compared a catalytic packed bed of seven hole cylinders with complex structures such as monolith and foam, keeping the geometric volume and surface area constant for all shapes. The monolith structure showed the lowest pressure drop, followed by the seven-hole cylinder and lastly by the foam structure due to the higher tortuosity of the structure. Similar studies comparing the performance, both technical and economic, of simpler geometries inspired from catalysis with more complex shapes would be of interest as these geometries can already be easily and cost effectively manufactured speeding up implementation.

As seen reported in literature, the separation performance as well as the cost is influenced by the geometries of the structured adsorbent. Optimal geometric parameters will provide the desired performance but a trade-off will still exist between minimizing pressure drop while improving the mass transfer and productivity. Therefore, cycle design studies and economic evaluations should also be performed to clearly understand the true potential of implementing structured sorbents is PSA systems.

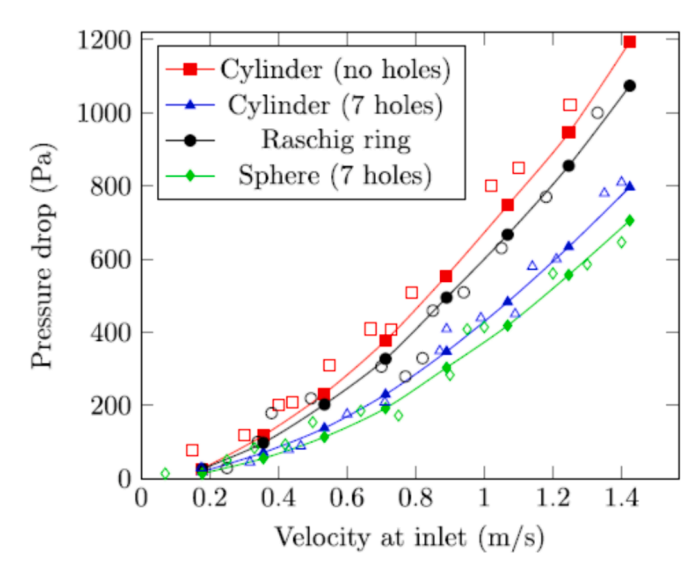


**Fig. 9.** Comparison of numerical and experimental data: the hollow points – experiment; the solid points and lines – CFD modelling. Reprinted with permission from Pashchenko [88].

Most of the research on shaped adsorbents focuses on lab-scale testing and there is limited information about what would be the performance of these structures when they go from lab to demonstration or industrial scale. Based on modelling and simulation, performance at large-scale can be estimated from relationships developed at lab-scale but these results should be validated experimentally. The effect of material shape and its size is scarcely investigated in the literature. It is expected that the shaping benefits will not scale linearly with size [42]. Another important factor to consider when scaling up from lab-scale is the sizing of the external piping to avoid additional pressure drop or void volume. Similarly, the loading of the structures in the column is not discussed in literature, although it is an essential part in advancing the technology. As mentioned in Section 2, there are currently two scale-up strategies proposed, stacking structures on top of each other or using multiple structures in the same reactor similar to multitubular reactors. As the technology advances allowing for more mechanically stable structures, single block or cartridge reactor structures may also become a possibility. Material stability in general is an important aspect regarding scale-up where adsorbents are needed to withstand a large number of cycles without needing replacement. Therefore, duration tests should be widely applied for any new or developed adsorbent.

# 4. Modelling

In order to design efficient adsorption processes, modeling plays a crucial role as it allows for fast and inexpensive evaluations. To do so, it is necessary to describe as accurately as possible the phenomena taking place inside the column. There are various studies concerning modeling of PSA processes [25,90,91]. Typically, the dynamic behavior of the adsorption process is described using a series of partial differential equations representing the mass, energy and momentum balances. The differences between models come from the specific ways of expressing pressure drop, mass transfer rate, heat transfer as well as the shape of the equilibrium isotherm. In the next sections, the influence of shaping on these phenomena is reviewed in more detail with the exception of the isotherm which is mainly material dependent.

Most reported correlations used for packed beds were developed for spherical particles [92,93]. For non-spherical particles an equivalent diameter is introduced with various definitions available. A comprehensive review can be found in [94]. The most commonly used ones are presented in Table 2. However, for more complex geometries the application of the equivalent diameter becomes more challenging as well as less accurate. In case of geometries with channels (e.g., monoliths) the hydraulic diameter is typically used. Formulas to evaluate the hydraulic diameter of circular, square, triangular and hexagonal channel geometries as a function of the monolith channel's characteristic length and the wall thickness can be adopted from work done on catalysts [95]. In general, computational fluid dynamics (CFD) is employed to assess important parameters such as the bed voidage and subsequently the pressure drop, mass and heat transfer in complex geometries without relying on experimental measurements.

 Table 2

 Equivalent diameters for non-spherical shapes.

Diameter name	Definition	Formula	
Surface volume (or Sauter) diameter	Diameter of a sphere of equal volume/surface area ratio as the particle	$d' = 6\frac{V_p}{A_p}$	Eq. (1)
Volume diameter	Diameter of a sphere of equal volume as the particle	d'' =	Eq. (2)
		$\left(\frac{6V_p}{\pi}\right)^{1/3}$	

#### 4.1. Pressure drop

The pressure drop (i.e., flow resistance) inside a packed bed of spheres has been reviewed extensively in literature [96,97]. The two most referenced correlations are those proposed by Ergun [98] and Carman [99]. Since their publishing more than 70 years ago, many correlations were set forward with claims of improved accuracy or range of applicability. A general way of representing the pressure drop is in the form of a dimensionless friction factor (f') which can be expressed as seen in Eq. (3) or as a function of the dimensionless Reynolds (Re) number (Eq. (4). Different forms of Re are used in literature as defined in Table 3 depending on how the velocity is expressed [100]. The most common one used in the expression of the friction factor is the modified Reynolds number, Re" described by Eq. (7) [97,101–103].

$$f = \frac{-\Delta P}{L} \frac{d_p}{\rho u_0^2} \frac{\varepsilon^3}{(1 - \varepsilon)}$$
 (3)

$$f = \left[\frac{150}{Re''} + 1.75\right] \frac{(1 - \varepsilon)}{\varepsilon^3} \tag{4}$$

A thorough literature review of friction factors inside a packed bed was performed by Erdim et al. [97], which not only collected the available correlations but also tested 38 of them using spherical particles of nine different sizes. Consequently a new correlation was formulated with improved accuracy for the parameter ranges assessed in their work 0.37  $<\epsilon<$  0.47, 4 < d<sub>t</sub>/d<sub>p</sub> < 34, and 2 < Re"<3600. Following the work of Erdim et al. [97], new correlation were published looking also at other shapes. Von Seckendorff et al. [101] proposed a revised Carman-type correlation for the pressure drop for equilateral cylinder packings valid for Re''=10-3000. The modified Re number, Re'', was used in the proposed friction correlation. Mohammadi et al. [104] proposed a methodology for developing 1-D axial pressure drop correlations for structured adsorbents with parallel channels based on 3D Navier-Stokes CFD modelling. The methodology was successfully validated for triangular shaped channels against experimental data as well as against two correlations previously proposed in literature. The range of validity is restricted to laminar flow regime with Re  $\leq$  2000.

In structures with channels (e.g., monoliths, laminates), the Hagen Poiseuille equation is typically used to evaluate pressure drop [15,61,104]. In fiber adsorbents Happel's cell model is generally employed [15,105], while for foam structures an Ergun-like equation [70] or a new equation proposed by Richardson et al. [67] can be used. Table 4 summarizes pressure drop correlations for the main geometries used in structured sorbents.

# 4.2. Bed void fraction

An important parameter in the calculation of the pressure drop is the bed void fraction. Low bed voidage is desired, even if it has a negative effect on the pressure drop, in order to reduce the column size [12] as well as to have a higher volumetric efficiency for increased throughput [107]. Bed voidage is greatly influenced by the shape of the particle. By changing the shape of the adsorbents, the bed voidage can be manipulated to lead to acceptable performance in terms of pressure drop. Tortuosity is another parameter that can influence the pressure drop. It

**Table 3**Reynolds number definitions.

Equation		Description
$Re = \frac{\rho \ d_p \ u_0}{\mu}$	Eq. (5)	Superficial gas velocity (u <sub>0</sub> )
$Re' = \frac{\rho \ d_p \ u_0}{\mu \ \varepsilon}$	Eq. (6)	Effective/interstitial gas velocity ( $u_0/\epsilon$ )
$Re^{"} = \frac{\rho \ d_p \ u_0}{\mu \ (1 - \varepsilon)}$	Eq. (7)	Modified Reynolds number

(16)

**Table 4**Pressure drop correlations used for structured packed beds.

Shape	$\Delta P$ correlation		
Spheres and Pellets	Ergun [98]	$rac{\Delta P}{L} = 150 rac{(1-arepsilon)^2}{arepsilon^3} \; rac{\mu \; u_0}{d_p^2} +$	Eq. (8)
		$1.75 \frac{(1-\varepsilon)}{\varepsilon^3}  \frac{\rho  u_0^2}{d_p}$	
	Carman [99]	$rac{\Delta P}{L} = 180 rac{\left(1-arepsilon ight)^2}{arepsilon^3} \; rac{\mu \; u_0}{d_p^2} +$	Eq. (9)
		$2.871 \frac{(1-\varepsilon)^{1.1}}{\varepsilon^3} \frac{\rho \ u_0^{1.9}}{d_0}$	
Monoliths and	Hagen	$\frac{\Delta P}{L} = \frac{32 \ \mu \ u_0}{\varepsilon \ d_z^2}$	Eq.
Laminates	Poiseuille	$\frac{1}{L} = \frac{1}{\varepsilon d_h^2}$	(10)
	[15,61,104]		
Fibers	Happel	$\frac{\Delta P}{I} =$	Eq.
	[86,106]	L μ 11 <sub>α</sub>	(11)
		$rac{r_{oD}^2 - 3r_{fs}^2}{8} + \ln\left(rac{r_{fs}}{r_{oD}} ight)rac{r_{fs}^4}{2\left(r_{fs}^2 - r_{oD}^2 ight)}$	
Foams	Richardson [67]	$\frac{\Delta P}{I} = \frac{(1-\varepsilon)^2}{c^3} \left( \mu \ u_0 \ \alpha \ \gamma^2 \right) +$	Eq.
		L e	(12)
		$\frac{(1-\varepsilon)}{\varepsilon^3} \left( \rho \ u_0^2 \ \beta \ \gamma \right)$	
		$\alpha = 973 \ d_p^{0.743} \ (1 - \varepsilon)^{-0.0982}$	
		$\beta = 368 \ d_p^{-0.7523} \ (1 - \varepsilon)^{0.07158}$	
		$\gamma = \frac{12.979 \left[ 1 - 0.971 (1 - \varepsilon)^{0.5} \right]}{d_{-} (1 - \varepsilon)^{0.5}}$	
		$d_p (1-arepsilon)^{0.5}$	

describes the complexity of the void space and has a direct influence also on the mass transport [108]. For structured adsorbents such as monoliths, laminates and fibers, the tortuosity is equal to 1, while in a conventional packed bed using beads can be 2–3, which means that lower pressure drops are achieved in a structured sorbed at the same voidage as a bed packed with beads for example [12]. Bulk void fraction correlations for a fixed bed containing spherical and equilateral solid and hollow cylinder packaging are presented by Dixon [109]. Predictions can be made to evaluate the voidage in case of equilateral hollow cylinders (Eq. (13) based on the correlations for solid cylinders (Eq. (14) and by considering a correction factor for internal voidage and interpenetration of packings, f (Eq. (15). With "a" being the inside diameter of the hollow cylinder and "b" the outer diameter.

$$\varepsilon_{hc} = \begin{cases} 1 - (1 - \varepsilon_{sc}) \left(1 - \frac{a^2}{b^2}\right) & for \frac{a}{b} < 0.5\\ 1 - f(1 - \varepsilon_{sc}) \left(1 - \frac{a^2}{b^2}\right) & for \frac{a}{b} \ge 0.5 \end{cases}$$

$$(13)$$

Where.

$$\varepsilon_{sc} = \begin{cases} 0.36 + 0.1 \frac{d^{"}}{d_{t}} + 0.7 \left(\frac{d^{"}}{d_{t}}\right)^{2} & for \frac{d^{"}}{d_{t}} \leq 0.6 \\ 0.677 - 9 \left(\frac{d^{"}}{d_{t}} - 0.625\right)^{2} & for 0.6 < \frac{d^{"}}{d_{t}} < 0.7 \end{cases}$$

$$1 - 0.763 \left(\frac{d^{"}}{d_{t}}\right)^{2} & for \frac{d^{"}}{d_{t}} \geq 0.7$$

$$(14)$$

$$f = 1 + 2\left(\frac{a}{b} - 0.5\right)^2 \left(1.145 - \frac{d}{d_t}\right) \tag{15}$$

Voidage correlations for randomly packed beds of various adsorbent shapes have also been determined experimentally by Benyahia and O'Neill [110]. The general expression represented by Eq. (16) is proposed to be valid for spheres, solid cylinders, hollow cylinders and 4-hole cylinders with an average error of 5.2 %. Column to particle diameter ratio  $(d_t/d_{p,\rm eq})$  is the main parameter involved in the voidage correlation. For non-spherical particles, the equivalent sphere diameter

 $(d_{p,eq})$  is used to describe non-spherical particles, however the definition of the used equivalent diameter is not specified in the reference.

$$arepsilon = \left(0.1504 + rac{0.2024}{arphi}
ight) + rac{1.0814}{\left(rac{d_t}{d_{p,eq}} + 0.1226
ight)^2} \quad ext{ for } < rac{d_t}{d_{p,eq}} < 50, ext{ and } \ < arphi < 1.0$$

With  $\phi$  being the sphericity

$$\varphi = \frac{\pi \ d_{p,eq}^2}{A_P} \tag{17}$$

As an alternative to the equivalent diameter, some correlations available in the literature are based on the particle sphericity instead. A summary can be found in the review prepared by von Seckendorff and Hinrichsen [92].

In the case of shapes with complex geometry there are not many universal correlations available. However, for catalytic applications complex shapes like monoliths with different geometry channels have been previously described and can be used or adapted for adsorption processes. Void fraction correlations for monoliths with circular, square, triangular or hexagonal shaped channels as a function of cell density, wall thickness and characteristic lengths of the monolith channel can be found in [95]. Similarly, porosity correlations for foam-based structures can be adapted from work done on catalyst structures (e.g., tetrakaidekahedral and diamond lattices) [111]. In their work, Mohammadi et al. [104] used Eq. (18) to validate the void fraction in a monolith structure with equilateral triangular straight channels in case of an adsorbent-coated structure. In case of complex geometries CFD is typically used, however CFD relies heavily on specific knowledge of the geometry of the system which is often not well defined.

$$\varepsilon = \frac{l}{\left(4\sqrt{3}\left(\delta_a + \frac{1}{2}\delta_w\right) + l\right)} \tag{18}$$

where,

$$l = \frac{2}{\sqrt{3}} \left[ -3\left(\delta_a + \frac{1}{2}\delta_w\right) + \left(9\left(\delta_a + \frac{1}{2}\delta_w\right)^2 + \frac{\sqrt{3}}{C_D}\right)^{1/2} \right]$$
 (19)

#### 4.3. Mass transfer

Mass transfer rate is an important parameter influencing the efficiency of the adsorption process. It depends on the length of the diffusion paths which is correlated to the type of pores available, their volume and size [107]. Besides average pore diameter and pore volume, other sorbent surface properties such as polarity, pH, functional groups, or roughness, can also influence the mass transfer of adsorbents with identical shapes. These properties are considered material dependent and will not be further addressed as it is out of the scope of the paper.

Mass transfer limitations are caused by external or internal diffusion. External diffusion takes place in the gas phase while internal diffusion happens in the adsorbent's pores. Short diffusion paths are desired for improved mass transfer rate. The influence of the various diffusion paths can be estimated by different characteristic numbers. The Biot number (Bi) shows the relative importance of internal versus external resistances and for mass transfer (Bi<sub>m</sub>) it is generally represented by Eq. (20) [112]. Typical magnitudes in case of sorbent systems for gas separation are Bi<sub>m</sub> $\gg$ 1. Internal resistances are dominant when Biot is large. For packed beds Bi<sub>m</sub> is in the range 5–500, thus the major resistance for mass transfer is in the particle and the external film resistance is negligible in case of pellets or foams [12,112]. In contrast, for structures such as laminates, monoliths and fibers, external film diffusion can be the

dominant resistance in case of large channel diameters and wall thicknesses [12].

$$Bi_m = \frac{0.357}{2 \varepsilon} \frac{D_m}{D_e} Re^{0.641} Sc^{\frac{1}{3}}$$
 for  $3 < Re < 2000$  (20)

The Sherwood (Sh) number describes the ratio of total mass transfer to external film diffusion and can be expressed as a function of the Reynolds and Schmidt numbers, Sh = f(Re, Sc). Table 5 lists the different definitions available for the Sh number depending on structure shape.

There are different mechanisms to describe internal diffusion depending on the type of pores present (e.g., macropores > 500 Å, mesopores 20–500 Å, micropores < 20 Å). In case of macro and mesopores, for large pore diameters with respect to the mean free path molecular diffusion is dominant, while in case of equal or smaller pores than the mean free path the Knudsen diffusions becomes dominant. Micropore diffusion becomes important in case of diffusing molecules have comparable diameters as the pores. [116]. Even though pore diffusion models give a more realistic description, their computation is quite complex. Thus, the Linear Driving Force (LDF) model proposed by Glueckauf [117] is generally applied in literature (Eq. (26) irrespective of the actual nature of the mass transfer resistance [116].

$$\frac{\partial \overline{q}}{\partial t} = k_{LDF} \ (q^* - \overline{q}) \tag{26}$$

The overall mass transfer coefficient,  $k_{LDF}$ , is dependent on the shape of the particle (see Table 6). For the model proposed by Glueckauf [117] which uses spherical particles,  $k_{LDF}$  is expressed by Eq. (27). Patton et al. [115] looked into the LDF approximation for various geometries with the goal of attaining a correlation suitable to be applied for the design of monolith structured adsorbents with different channel geometries. Applying the method proposed by Liaw et al., [118] which demonstrated that  $k_{LDF}$  can be easily determined by assuming a parabolic concentration profile in the pellet (Eq. (32), Patton et al. [115] was able to formulate  $k_{LDF}$  expressions for more complex channel geometries (e.g. square, rectangular, triangular, hexagonal) based on the  $k_{LDF}$  approximation for hollow cylinder with insulated external surface. In Eq. (32),  $a_0$  and  $a_2$  are functions of time and axial distance and do not depend on the radial distance from center of particle, R.

$$q = a_0 + a_2 R^2 (32)$$

Axial dispersion is caused by molecular diffusion and turbulent mixing

 Table 5

 External film diffusion in structured packed beds.

Shape	Sh number definition		Range of validity	References
(Single) Sphere	$Sh = 2 + 0.6 Re^{0.5} Sc^{0.33}$	Eq. (21)	$1 < Re < 10^4$	[55]
Pellets	$Sh = 2 + 1.1 Re^{0.6} Sc^{0.33}$	Eq. (22)	$3 < Re < 10^4$	[113]
Foam	$Sh = 0.91 \ Re^{0.43} \ Sc^{0.33}$	Eq. (23)	15 < Re < 200	[114]
Monolith Laminate	$Sh = A \left( 1 + B \ Re \ Sc \ rac{d_h}{l}  ight)^{0.81}$	Eq. (24)	Re < 500 Chanel type: Circular: A = 3.6 Triangular: A = 2.35 Square: A = 2.95 B = channel roughness constant	[71,115]
Fiber	$Sh = 1.45 \left( Re \ Sc \ \frac{d_{f,out}}{l} \right)^{0.33}$	Eq. (25)	Laminar regime on shell-side	[86,106]

and it is neglected for conventional fixed beds in most cited literature since mass transfer resistances are significantly greater [112,116]. However, for particles smaller than 1 mm or low linear gas velocity, it can have a more significant contribution outweighing the benefits to the kinetic effects [12]. In case of structured adsorbents the flow characteristics are different due to much higher bed voidage which leads to stronger dispersion effects influencing the breakthrough front and as a result the separation effectiveness [71,120]. The axial diffusion coefficient (Dz) is typically expressed in term of Péclet number (Pé) as represented in Eq. (33). The Péclet number is described a function of Reynolds and Schmidt numbers using Eq. (34) [112].

$$Pe = \frac{u_0 \ d_p}{D_c} \tag{33}$$

$$\frac{1}{p_e'} = \frac{0.3}{Re \ Sc} + \frac{0.5}{1 + \frac{3.8}{Re \ Sc}} \quad for \quad < Re < 400$$
 (34)

In case of monoliths and laminates, axial dispersion coefficients can be approximated from correlations describing flow in pipes [120]. Specific corelations of axial dispersion in fiber adsorbent beds are not present in literature, thus as an approximation Eq. (35) was used by Sen et al. [86] in their study (see Table 7).

Improved mass-transfer and lower pressure drop are especially relevant during regeneration. As regeneration is often performed at low pressure, the reduction of pressure drop is especially impactful here. In the case of systems with a purge feed, the reduced pressure drop allows for high purge flow rates. While an improved access to the adsorption sites improves the desorption kinetics.

#### 4.4. Heat transfer

Heat effects are a consequence of the sorption enthalpy. Generally, adsorption processes are assumed isothermal with the heat generated during the exothermic adsorption step not having a significant influence on the performance of the system. In practice this is not always valid as temperature increase has a negative effect on the adsorption capacity and influences the loading during cyclic operation, an effect which can be pronounced especially in the case of relatively concentrated adsorbate streams [121]. Similarly, during regeneration the sorbent is cooled by the desorption process which deteriorates system performance.

Similarly to mass transfer, heat transfer resistance is also influenced by the various diffusion paths. The heat-Biot number (Bi\_h) is represented by Eq. (38) [112] as a function of Re and Prandtl number (Pr) instead of Sc. Typical magnitudes of heat-Biot number are  $\mathrm{Bi}_h < 1$  which means that contrary to mass transfer, the major resistance for heat transfer, in case of pellets or foams, is in the external film. Nusselt number (Nu) is the heat transfer analogue of the Sherwood number, thus external film diffusion is expressed using similar correlations as presented in Table 5 replacing Sc with Pr.

$$Bi_h = \frac{0.357}{2\varepsilon} \frac{k_g}{k_e} Re^{0.641} Pr^{\frac{1}{3}} \quad for \quad < Re < 2000$$
 (38)

The effect of adsorbent shaping on the heat transfer was studied by Rezaei and Grahn [122] for different adsorbent structures (e.g., monoliths, laminates, foam and pellets) under isothermal, adiabatic and nonadiabatic conditions. For nonisothermal conditions it was shown that the temperature rise has also an influence on the adsorption, leading to less sharp and faster breakthroughs. In case of monoliths, high cell densities were shown to lead to lower and more uniform bed temperatures. Similarly for foam adsorbents, increased pore densities are preferred for the same effect. In case of laminates small sheet spacing are desired for a more efficient heat dissipation. All evaluated adsorbent structures showed a smaller temperature gradient inside the column compared to the conventional packed bed of pellets, due to an improved effect thermal conductivity in the bed. In particular, the possibility to

**Table 6** K<sub>LDF</sub> definitions used in structured packed bed.

Shape	$k_{ m LDF}$ definition		Ref
Sphere	$k_{LDF}=15  rac{D_e}{r_c^2}$	Eq. (27)	[115]
Pellets	$k_{LDF}=8~rac{D_e^{r}}{r_p^2}$	Eq. (28)	[115]
Monolith	Hollow cylinder with insulated external surface:	Eq. (29)	[115]
	$k_{LDF} = \frac{4}{\left[\left(\frac{r_o}{r_i} - 1\right)(r_o^2 - r_i^2) - \frac{1}{r_i(r_o - r_i)}\right] \left[\frac{1}{2}(r_o^4 - r_i^4) - \frac{4r_o}{3}(r_o^3 - r_i^3) + r_o^2(r_o^2 - r_i^2)\right]}$		[110]
Laminate	$k_{LDF} = D_e$ l	Eq. (30)	[119]
Fiber	$k_{LDF} = 8 \; rac{D_e \; r_{0D}^2}{r_{oD}^2 - r_{iD}^2}$	Eq. (31)	[86]

**Table 7**Axial dispersion in packed beds.

Shape	Equation		Range of validity	References
Spheres/ Pellets Foam, Fibers	$D_z = rac{D_m}{arepsilon}(20 + 0.5~Sc~Re)$	Eq. (35)	Laminar regime	[71,86,112]
Monolith/ Laminate	$D_z = D_m + rac{1}{192} rac{u_0^2}{D_m} rac{d_h^2}{D_m}$ or $rac{D_z}{u_0} = rac{1}{L} = rac{Re\ Sc}{192}$	Eq. (36) or Eq. (37)	Laminar regime	[71,120]

introduce a thermally conductive support structure can be beneficial.

Heat-exchanger configurations have been proposed to deal with the heat effects, essentially balancing the heat of adsorption and desorption [121,123]. Lee et al. [124] have proposed a heat exchanger design for H<sub>2</sub> purification, where a cylindrical bed was surrounded by an annular bed, that led to an improvement in performance. For full-scale application, the use of a large heat exchange surface area seems important. More recently, the use of plates-type heat exchange configurations has been proposed for PSA operations by Shabbani et al. [125,126]. Sorbent shaping techniques could expedite this promising development, as they can enable the adoption of sorbent shapes that enable heat transfer by a high effective bulk thermal conductivity. Similar effects have indeed been recently presented for 3D printed 'logpile' structures that provide a more lenient heat transfer - pressure drop trade-off sin heterogeneous catalysis [127]. Moreover, the potential for improved mass transfer (as discussed in Section 4.3 above) will allow to minimize the wall effect in these designs that require relatively large surface areas for heat exchange. Besides the use of heat exchangers, phase change materials have been proposed to deal with the heat of adsorption. As discussed above, covalent organic framework (COF) adsorbents can provide high thermal conductivities [128]. Ma et al [129] have reported ultra-high thermal conductivity (>15 W m<sup>-1</sup> K)) for COF-300 although a strong function of the nanometer-range pore size. In order to make use of the enhanced intrinsic thermal conductivity of adsorbent materials, research into the shaping of these adsorbents is needed to either increase the bed solid density or create effective paths for conduction, in order to arrive at a high effective macroscopic thermal conductivity as well. Thus, sorbent shaping can contribute to the development of non-adiabatic adsorption systems, by improving the mass transfer (reducing the wall effect, improving flow characteristics, increasing sorbent bulk density) as well as heat transfer (bulk thermal conductivity).

#### 4.5. Productivity

Besides low pressure drop and high mass transfer kinetics, an ideal PSA process should also allow for high productivities. Productivity is defined as the amount of product obtained per unit volume or mass of adsorbent in a unit of time [130]. Developed dimensionless scaling rules for improving the system productivity [131,132] depend on rate limiting steps in mass and heat transfer, rather than a particular system layout. The rules define a system of solutions for which dimensionless temperature, concentration, and pressure remain the same. As such, they are applicable to intensification of adsorption processes by sorbent shaping, provided that adapted relationships are implemented (cf. Sections 4.1-4.4). Importantly, however, shaped sorbents are able to provide the highest impact by their ability to change the relationship between temperature, concentration, and pressure. This means the system would require a case by case redesign rather than the use of scaling rules. As this is inherently computationally intensive, this is also where advanced numerical techniques will exert a significant impact.

Productivity is one property which often suffers when adopting structured adsorbents as the volumetric loading of the adsorbent bed is generally lower compared to conventional geometries such as beads or pellets [12]. High working capacities, high adsorbent loading, and short cycle times are desired if the aim is to increase the productivity which can be expressed by Eq. (39) [71].

Productivity = 
$$k \frac{WC}{\tau} = k \frac{WC - f(\Delta P) - f(MTZ)}{\tau}$$
 (39)

where, k is a proportionality constant, WC is the working capacity,  $\tau$  is the cycle time, and  $f(\Delta P)$  and f(MTZ) are functions of pressure drop and mass transfer zone, respectively. The working capacity, expressed as amount of gas adsorbed or desorbed per mass or volume adsorbent [71], is directly related to the material and the operating conditions of the system being negatively influenced by the pressure drop (reducing the pressure swing). The mass transfer zone can also negatively impact the productivity by the reduction of the bed's effective length which also correlates to a reduction in working capacity. High adsorbent densities together with low bed voidage are desired in case of rapid cycling in order to minimize losses during pressurization/depressurization. In standard pellet PSA processes about twice the amount of gas is adsorbed compared to the void fraction of the bed. When using shaped sorbents with higher void fraction the void-to-sorbent ratio increases and more energy/gas is needed to repressurize the columns compared to what is adsorbed [12]. Short cycle times can be achieved by an increase in flowrate which means also higher velocities. As a consequence increased void fractions and surface area are desired to limit pressure drops and subsequently energy consumption. As seen, increasing productivity of a PSA system is not that straightforward as it depends on many interrelated factors. Fig. 10 illustrates the influence of adsorbent shaping on the specific productivity. It clearly shows that the redesign of a PSA cycle with the use of a structured adsorbent leads to improved performance, surpassing conventional tradeoffs between bed density (amount of sorbent (kg) per m<sup>3</sup> of column) and pressure drop, particle density and mass transfer limitations. It is interesting to note that for all shapes evaluated, there is an optimum where the productivity is the highest. Outside this

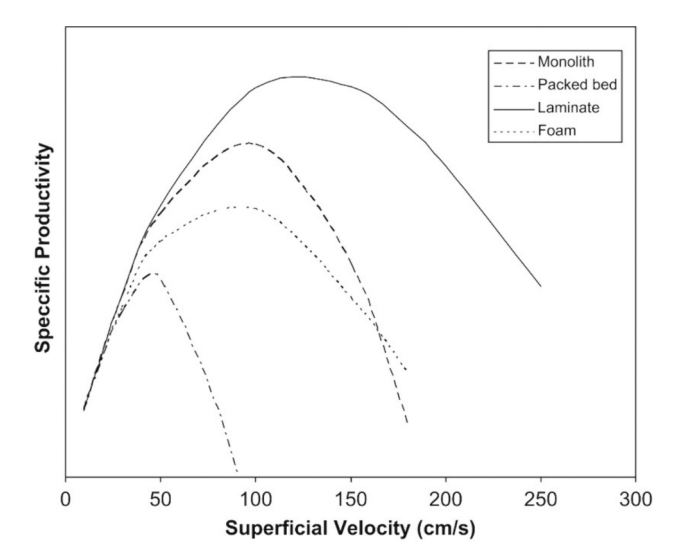


**Fig. 10.** Specific productivity versus superficial velocity: structured adsorbents (monolith, laminate, foam) enable new cycle designs with increased specific productivity. Figure reprinted with permission from Rezaei and Webley (2009) [71].

optimum condition, reduced productivity is observed also for structured sorbents.

In terms of cycle design, the reduction of pressure drop allows for reduction of the regeneration pressure improving the working capacity. As the WC depends on the material and its isotherm, different isotherms lead to different operations. A material with a linearly increasing isotherm can be operated at any pressure level and increasing the pressure difference between adsorption and desorption increases the WC. For materials with Langmuir-like isotherms, the steepest increase in loading is in the lower partial pressure range while at higher pressure ranges, the isotherm levels off. As such a pressure swing between high pressures will not lead to a high WC while going to (shallow) vacuum can significantly increase the WC [133]. At (shallow) vacuum pressures the gas velocities and the resulting pressure drops increase rapidly thus making shaping necessary to achieve a rapid regeneration. A lower adsorption pressure can be applied when shaping and lower regeneration pressure come together, as these lead to deeper regeneration of the sorbent and lower pressure drop during adsorption, while the WC is not significantly affected for materials with Langmuir-like isotherms [134].

As a result, optimization of the PSA cycle is essential to make sure all the advantages offered by using structured adsorbents are fully exploited.

# 4.6. Artificial intelligence: New methods for improved cycle design

Modeling of PSA systems makes use of second order partial differential and algebraic equations (PDAE) to describe the phenomena of the process. Generally PDAEs are converted into differential-algebraic equations (DAE) or algebraic equations (AE) to be solved by different solvers which are generally complicated and time-consuming making optimization of the system quite challenging [90]. In addition, the complexity of PSA optimization is also brought about by its cyclic behavior and the fact that it employs multiple steps – each with different characteristics taking place in different columns while the process targets multiple performance indicators (e.g., product purity and recovery, productivity, and energy consumption) which are influenced by various input parameters (e.g., temperature, pressure, flowrate, column size, cycle time, number of steps etc.) often leading to complex tradeoffs [135]. Like in other fields of chemical engineering, machine learning methods have been successfully applied to simplify and speed up optimization of these complex systems. For a more general overview of techniques, the reader is referred to excellent reviews available in literature [136–141].

One of the main advantages of these kind of models is their speed, making optimization and control of PSA systems much easier to implement. Compared to the detailed models, the main drawback of surrogate models is the fact that they cannot be extrapolated to cover other conditions/configurations outside the scenarios used for training. Therefore, flexibility to allow for multiple combinations of the steps in the cycle design needs to be the focal point when developing these models.

Multi-objective optimization of a six-step two-bed PSA system for H2 purification was carried out based on artificial neural networks (ANN) by Tong et al. [142]. Based on known operating conditions such as adsorption pressure and step time, the ANN was successfully trained to accurately predicted hydrogen recovery and purity and to optimize the performance of the system. Similar study was carried out by applying ANN and polynomial regression models by Xiao et al. [143]. It was found that ANN models could more accurately achieve the desired outputs under different weights. Two optimization approaches based on machine learning methods, surrogate-assisted and design space dimensionality reduction, were evaluated by Subraveti et al. [144] in case of a 8-step PSA process for CO<sub>2</sub> capture. Reduction in computational time of about one order of magnitude was observed while still maintaining the performance of the original detailed model. Oliveira et al. [145] evaluated the performance of two other methods, ANNs and deep neural networks (DNN), for the optimization of the H<sub>2</sub>/CO ratio in case of a PSA process for syngas pre-treatment downstream Fischer-Tropsch process. Better performance was generally observed for the DNN models which were able to predict the dynamic behavior of the PSA with higher precision. Beyond performance targets such as purity and recovery, Martins et al. [146] looked into simultaneous economic optimization and advanced control strategies for a PSA unit for syngas purification based on DNN models. Techno-economic optimization of a PSA system for CO2 removal considering two cases and different adsorbent materials was evaluated by Andersson et al. [147]. Bayesian optimization and other two optimization algorithms presented in literature were employed on a reduce-order PSA model showing good results in terms of reliability and computational time. Li et al. [148] combined generic algorithms with ANN to perform multi-objective optimization of CO and CH<sub>4</sub> breakthrough times and operating conditions for a hydrogen purification PSA system. For predicting breakthrough curves, the authors advise for the use of more complex algorithms such as DNNs. Optimization under constraints of a PSA system for integrated H<sub>2</sub> purification and CO<sub>2</sub> capture, applying ANN models, was performed by Streb and Mazzotti [149]. The authors draw attention to the poor accuracy of the ANN model for conditions found at the boundary of the sampling domain and recommend to avoid using the models in this region or increasing the number of training data for these regions. Pai et al. [150] compared the performance of various machine learning algorithms (i.e., decision tree, random forest, ANN, Gaussian process regression, support vector machines) for the multi-objective optimization of a VSA process for CO<sub>2</sub> capture. For a fixed set of operating conditions, Gaussian process regression-based surrogate models showed the best predictions with the smallest number of training data points. In addition, the authors also used an ANN-based model to predict cyclic steady state and used it to speed-up convergence of the detailed model. Simultaneous optimization of process conditions and adsorbent selection was performed by Kim et al. [151] for a VPSA system intended for post-combustion CO<sub>2</sub> capture considering 75 adsorbent materials and 5 operating conditions. Two surrogate-based optimization approaches were compared in terms of accuracy and computational time - nonlinear programming (NLP) and mixed-integer nonlinear programming (MINLP), with the latter proving to be more efficient. Simultaneous optimization of process conditions and adsorbents screening was extensively studied by various authors [152–158], nonetheless the influence of adsorbent shaping was not considered so far in optimization problems.

Data-driven models most commonly known as surrogate models,

machine learning models, or meta-models, are black-box models which approximate the solution of a detailed model based on its input-output relationships data. A new emerging branch of machine learning techniques is physics-informed neural networks (PINN) which uses ANN to solve PDEs [159]. In this approach conservation equations are included as constraints. It has been successfully applied to various areas of chemical engineering, such as fluid mechanics [160] or heat transfer [161]. A first attempt at applying this method for adsorption systems was done by Santana et al. [162] showing that PINNs are efficient in solving the PDE describing the system and subsequently used for parameter estimations. Following this, PINN were also applied to describe kinetics (breakthrough curves) [163] and adsorption equilibria [164] of chromatographic processes. In an interesting example of combining data-driven and physical models, Leperi et al. [165] developed (data-driven) surrogate models for each of the most common steps of a PSA cycle using data from three different cycles design (e.g., 3, 4 and 5 step designs) for training the ANN. The main advantage of their approach is the flexibility of evaluating different (physical) cycle designs by combining the ANN models of the desired steps. The developed model was used to evaluate the optimization of a PSA cycle for CO<sub>2</sub> capture considering two different adsorbent materials (i.e., MOF and Zeolite) showing good agreement compared to the rigorous PSA model at a reduction in computational time of approximately 3 orders of magnitude. Vo et al. [166] proposed a similar approach to the optimization of an integrated process for H<sub>2</sub> recovery and CO<sub>2</sub> capture from the tail gas of hydrogen plants. ANN was used to model the main units of the process (e.g., PSA unit, membrane, cryogenic) and subsequently integrate it with AEs to describe compressors, heat exchangers and to evaluate the economics of the entire process.

Most focus has been on optimization and control of existing systems. In view of the complex nature of PSA-type processes, hybrid approaches between physical models and data-driven models as well as PINNs seem to provide interesting opportunities, especially for the development of novel, optimized cycles for structured adsorbents.

# 5. Conclusions and outlook

Adsorbent shaping has been well established as an important enabler for intensified pressure swing adsorption (PSA) processes. Intensification of PSA cycles can be facilitated by structured adsorbents, for which reduced pressure drop and enhanced mass transfer kinetics have been well demonstrated experimentally as well as corroborated in modelling. Moreover, a major potential for further improvement can still be explored by redesigning the PSA system based on shaped sorbents, to allow in the end unsurpassed gains in productivity. In this context, only few papers have explicitly focused on productivity increase by cycle redesign [13,58,71,86]. For redesigning the PSA systems, it is of crucial importance that the set of available, validated model relations as outlined in this work become more widely established. In this paper, an attempt has been made to present a structured overview of model relations.

Desired properties for structured adsorbents were found to be high adsorbent loading in case of coated structures or with the use of binders, high bed density, high surface area, optimum bed voidage. For each structure, trade-offs to satisfy both high mass transfer and low pressure drop need to be identified to unlock full potential of implementing rapid cycling in PSA systems. The most important trade-off for each application depends on the process integration, and is a conclusion from technoeconomic analysis on a system level. Optimum geometric parameter ranges (e.g., wall thickness, cell density) found through modeling should also be validated at scales beyond lab-scale. In addition, in order to be applied industrially, structured adsorbents need to possess good mechanical and cyclic stability as well as long lifetimes. Thus, duration tests should be performed for newly developed structured adsorbents, providing valuable information for cost assessment as well. From the manufacturing part, easy, fast and cost-effective options are required.

Additive manufacturing, or 3D printing, has been identified as a promising shaping technique but there are still barriers to overcome for large-scale production. Simpler geometries inspired from catalysis (e.g., multi-hole cylinders, multi-lobe shapes) remain of interest, as these geometries can already be easily and cost effectively manufactured speeding up implementation. It is essential that the intensified PSA cycles are validated in pilots and demonstration units to corroborate the predicted performance gains.

Optimization of cycle design, not just of the geometric parameters, is essential to ensure that the benefits associated to shaping are completely exploited. There is limited information regarding the performance of structured adsorbents at realistic cyclic operation. Process dynamics will be different compared to the conventionally shaped material as a consequence of different mass transfer limitation (molecular diffusion vs film transfer). Artificial intelligence-based optimization methods. already extensively applied for PSA modeling and optimization, will bring a lot of opportunity for studying improved cycle designs. Performance evaluations should go beyond pressure drop, separation recovery and productivity and include also potential energy efficiency and size reduction compared against existing PSA systems in a systematic way so that even different geometric structures can be easily compared against each other for a specific application. Furthermore, techno-economic assessment has been scarcely evaluated so far [60,61,81]. More effort needs to be invested towards this to actually weight in the benefits of using structured adsorbents and thus take the next step towards implementation.

In conclusion, sorbent shaping provides the ability to fundamentally redesign and optimize pressure swing adsorption cycles. Based on our analysis, we highlight several complementary elements that will expedite the development of next generations of PSA systems:

- High-density and low pressure drop sorbents will be developed using the combined effort of experimental shaping efforts and numerical modelling techniques (including computational fluid dynamics).
   Especially for the latter, the use of artificial intelligence will enable relatively fast convergence.
- Taller and more slender columns will be made possible that improve the productivity.
- Low operating pressures will become feasible, both in the adsorption step and in the regeneration, leading to a better separation performance and improve efficiency. New cycle designs employing a (mild) vacuum for regeneration will become technically feasible.
- Because of the reduced column size, a larger number of columns per train will be economically attractive. This means systems will run more close to ideal 'countercurrent' operation (see also Sivakumar and Rao [167]) In the design and optimization, the use of artificial intelligence will also play an essential role.

Thus, sorbent shaping is a very promising developing field, that will reach its full potential if a more comprehensive approach will be followed.

#### CRediT authorship contribution statement

**Dora-Andreea Chisăliță:** Writing – original draft, Conceptualization. **Jurriaan Boon:** Writing – review & editing, Supervision, Conceptualization. **Leonie Lücking:** Writing – review & editing.

# Declaration of competing interest

The authors declare that they have no known competing financial interests or personal relationships that could have appeared to influence the work reported in this paper.

#### Data availability

No data was used for the research described in the article.

#### Acknowledgements

This project has received funding from the Dutch Ministry for Economic Affairs and Climate Policy.

#### References

- H.-J. Bart, U. von Gemmingen, Adsorption, Ullmann's Encycl. Ind. Chem. (2005), https://doi.org/10.1002/14356007.b03\_09.pub2.
- [2] L. Riboldi, O. Bolland, Overview on Pressure Swing Adsorption (PSA) as CO2 capture technology: state-of-the-art, limits and potentials, Energy Procedia 114 (2017) 2390–2400, https://doi.org/10.1016/j.egypro.2017.03.1385.
- [3] J. James, L.E. Lücking, H.A.J. van Dijk, J. Boon, Review of technologies for carbon monoxide recovery from nitrogen- containing industrial streams, Front. Chem. Eng. 5 (2023). https://www.frontiersin.org/articles/10.3389/fceng.2023. 1066.091
- [4] L.G. Oliveira, P.A. Cremonez, B. Machado, E.S. da Silva, F.E.B. Silva, G.C. G. Corréa, T.F.M. Lopez, H.J. Alves, Updates on biogas enrichment and purification methods: a review, Can. J. Chem. Eng. 101 (2023) 2361–2390, https://doi.org/10.1002/cjce.24671.
- [5] J. Boon, Sorption-enhanced reactions as enablers for CO2 capture and utilisation, Curr. Opin. Chem. Eng. 40 (2023) 100919, https://doi.org/10.1016/j. coche.2023.100919.
- [6] A.M. Parvez, S. Hafner, M. Hornberger, M. Schmid, G. Scheffknecht, Sorption enhanced gasification (SEG) of biomass for tailored syngas production with insitu CO2 capture: current status, process scale-up experiences and outlook, Renew. Sustain. Energy Rev. 141 (2021) 110756, https://doi.org/10.1016/j. rser.2021.110756.
- [7] S. Masoudi Soltani, A. Lahiri, H. Bahzad, P. Clough, M. Gorbounov, Y. Yan, Sorption-enhanced steam methane reforming for combined CO2 capture and hydrogen production: a state-of-the-art review, carbon capture, Sci. Technol. 1 (2021) 100003, https://doi.org/10.1016/j.ccst.2021.100003.
- [8] J. van Kampen, J. Boon, F. van Berkel, J. Vente, M. van Sint Annaland, Steam separation enhanced reactions: review and outlook, Chem. Eng. J. 374 (2019) 1286–1303, https://doi.org/10.1016/j.cej.2019.06.031.
- [9] J. Boon, P.D. Cobden, H.A.J. van Dijk, M. van Sint Annaland, High-temperature pressure swing adsorption cycle design for sorption-enhanced water-gas shift, Chem. Eng. Sci. 122 (2015) 219–231, https://doi.org/10.1016/j. ces.2014.09.034.
- [10] A. Mosca, J. Hedlund, F.N. Ridha, P. Webley, Optimization of synthesis procedures for structured PSA adsorbents, Adsorption. 14 (2008) 687–693, https://doi.org/10.1007/s10450-008-9126-9.
- [11] S. Lawson, X. Li, H. Thakkar, A.A. Rownaghi, F. Rezaei, Recent advances in 3D printing of structured materials for adsorption and catalysis applications, Chem. Rev. 121 (2021) 6246–6291, https://doi.org/10.1021/acs.chemrev.1c00060.
- [12] F. Rezaei, P. Webley, Structured adsorbents in gas separation processes, Sep. Purif. Technol. 70 (2010) 243–256, https://doi.org/10.1016/j. seppur.2009.10.004.
- [13] I. Sharma, D. Friedrich, T. Golden, S. Brandani, Monolithic adsorbent-based rapid-cycle vacuum pressure swing adsorption process for carbon capture from small-scale steam methane reforming, Ind. Eng. Chem. Res. 59 (2020) 7109–7120, https://doi.org/10.1021/acs.iecr.9b05337.
- [14] V.-C. Sandu, A.-M. Cormos, I.-D. Dumbrava, A. Imre-Lucaci, C.-C. Cormos, R. de Boer, J. Boon, S. Sluijter, Assessment of CO2 capture efficiency in packed bed versus 3D-printed monolith reactors for SEWGS using CFD modeling, Int. J. Greenh. Gas Control. 111 (2021) 103447, https://doi.org/10.1016/j. ijgec.2021.103447.
- [15] S.J.A. DeWitt, A. Sinha, J. Kalyanaraman, F. Zhang, M.J. Realff, R.P. Lively, Critical comparison of structured contactors for adsorption-based gas separations, Annu. Rev. Chem. Biomol. Eng. 9 (2018) 129–152, https://doi.org/10.1146/ annurev-chembioeng-060817-084120.
- [16] G. Zhong, D. Liu, J. Zhang, The application of ZIF-67 and its derivatives: adsorption, separation, electrochemistry and catalysts, J. Mater. Chem. A 6 (2018) 1887–1899, https://doi.org/10.1039/C7TA08268A.
- [17] I. Ahmed, S.H. Jhung, Applications of metal-organic frameworks in adsorption/ separation processes via hydrogen bonding interactions, Chem. Eng. J. 310 (2017) 197–215, https://doi.org/10.1016/j.cej.2016.10.115.
- [18] Y.R. Tao, H.J. Xu, A critical review on potential applications of Metal-Organic frameworks (MOFs) in adsorptive carbon capture technologies, Appl. Therm. Eng. 236 (2024) 121504, https://doi.org/10.1016/j.applthermaleng.2023.121504.
- [19] A. Abdelrasoul, H. Zhang, C.-H. Cheng, H. Doan, Applications of molecular simulations for separation and adsorption in zeolites, Microporous Mesoporous Mater. 242 (2017) 294–348, https://doi.org/10.1016/j.micromeso.2017.01.038.
- [20] E. Pérez-Botella, S. Valencia, F. Rey, Zeolites in adsorption processes: state of the art and future prospects, Chem. Rev. 122 (2022) 17647–17695, https://doi.org/ 10.1021/acs.chemrev.2c00140.
- [21] M. Asadollahzadeh, R. Torkaman, M. Torab-Mostaedi, Extraction and separation of rare earth elements by adsorption approaches: current status and future trends,

- Sep. Purif. Rev. 50 (2021) 417–444, https://doi.org/10.1080/15422119.2020.1792930.
- [22] R.P.P.L. Ribeiro, C.A. Grande, A.E. Rodrigues, Electric swing adsorption for gas separation and purification: a review, Sep. Sci. Technol. 49 (2014) 1985–2002, https://doi.org/10.1080/01496395.2014.915854.
- [23] M. Karimi, M. Shirzad, J.A.C. Silva, A.E. Rodrigues, Carbon dioxide separation and capture by adsorption: a review, Environ. Chem. Lett. 21 (2023) 2041–2084, https://doi.org/10.1007/s10311-023-01589-z.
- [24] R. Ben-Mansour, M.A. Habib, O.E. Bamidele, M. Basha, N.A.A. Qasem, A. Peedikakkal, T. Laoui, M. Ali, Carbon capture by physical adsorption: materials, experimental investigations and numerical modeling and simulations – a review, Appl. Energy. 161 (2016) 225–255. https://econpapers.repec.org/RePE c:eee:appene:v:161;y:2016;i:c:p:225-255.
- [25] M.S. Shafeeyan, W.M.A. Wan Daud, A. Shamiri, A review of mathematical modeling of fixed-bed columns for carbon dioxide adsorption, Chem. Eng. Res. Des. 92 (2014) 961–988, https://doi.org/10.1016/j.cherd.2013.08.018.
- [26] S. Cao, F. (Feng) Tao, Y. Tang, Y. Li, J. Yu, Size- and shape-dependent catalytic performances of oxidation and reduction reactions on nanocatalysts, Chem. Soc. Rev. 45 (2016) 4747–4765, https://doi.org/10.1039/C6CS00094K.
- [27] F. Zaera, Designing sites in heterogeneous catalysis: are we reaching selectivities competitive with those of homogeneous catalysts? Chem. Rev. 122 (2022) 8594–8757, https://doi.org/10.1021/acs.chemrev.1c00905.
- [28] C. Parra-Cabrera, C. Achille, S. Kuhn, R. Ameloot, 3D printing in chemical engineering and catalytic technology: structured catalysts, mixers and reactors, Chem. Soc. Rev. 47 (2018) 209–230, https://doi.org/10.1039/C7CS00631D.
- [29] E. Tronconi, G. Groppi, C.G. Visconti, Structured catalysts for non-adiabatic applications, Curr. Opin. Chem. Eng. 5 (2014) 55–67, https://doi.org/10.1016/j. coche.2014.04.003.
- [30] G. Zhao, J.A. Moulijn, F. Kapteijn, F.M. Dautzenberg, B. Xu, Y. Lu, Monolithic fiber/foam-structured catalysts: beyond honeycombs and micro-channels, Catal. Rev. (2023) 1–81, https://doi.org/10.1080/01614940.2023.2240661.
- [31] K.A. Cychosz, R. Guillet-Nicolas, J. García-Martínez, M. Thommes, Recent advances in the textural characterization of hierarchically structured nanoporous materials, Chem. Soc. Rev. 46 (2017) 389–414, https://doi.org/10.1039/ C6CS00391E.
- [32] X.-Y. Yang, L.-H. Chen, Y. Li, J.C. Rooke, C. Sanchez, B.-L. Su, Hierarchically porous materials: synthesis strategies and structure design, Chem. Soc. Rev. 46 (2017) 481–558, https://doi.org/10.1039/C6CS00829A.
- [33] P.P. Pescarmona, Modern Synthesis Routes to Hierarchically-Structured Porous Materials, in: Handb. Porous Mater., WORLD SCIENTIFIC, 2020, pp. 149–176. doi: doi: 10.1142/9789811223389\_0002.
- [34] M.-H. Sun, S.-Z. Huang, L.-H. Chen, Y. Li, X.-Y. Yang, Z.-Y. Yuan, B.-L. Su, Applications of hierarchically structured porous materials from energy storage and conversion, catalysis, photocatalysis, adsorption, separation, and sensing to biomedicine, Chem. Soc. Rev. 45 (2016) 3479–3563, https://doi.org/10.1039/ C6CS00135A.
- [35] Y. Zhu, P. Xu, X. Zhang, D. Wu, Emerging porous organic polymers for biomedical applications, Chem. Soc. Rev. 51 (2022) 1377–1414, https://doi.org/10.1039/ D1CS00871D
- [36] A. Henrique, H. Steldinger, J.L.D. de Tuesta, J. Gläsel, A.E. Rodrigues, H. T. Gomes, B.J.M. Etzold, J.A.C. Silva, Separation of alkane isomers in a hierarchically structured 3D-printed porous carbon monolith, Chem. Eng. J. 472 (2023) 145138, https://doi.org/10.1016/j.cej.2023.145138.
- [37] L.R.S. Rosseau, V. Middelkoop, H.A.M. Willemsen, I. Roghair, M. van Sint Annaland, Review on Additive Manufacturing of Catalysts and Sorbents and the Potential for Process Intensification, Front. Chem. Eng. 4 (2022). https://www. frontiersin.org/articles/10.3389/fceng.2022.834547.
- [38] H. Li, A. Dilipkumar, S. Abubakar, D. Zhao, Covalent organic frameworks for CO2 capture: from laboratory curiosity to industry implementation, Chem. Soc. Rev. 52 (2023) 6294–6329, https://doi.org/10.1039/D2CS00465H.
- [39] S. Cui, A. Marandi, G. Lebourleux, M. Thimon, M. Bourdon, C. Chen, M. I. Severino, V. Steggles, F. Nouar, C. Serre, Heat properties of a hydrophilic carboxylate-based MOF for water adsorption applications, Appl. Therm. Eng. 161 (2019) 114135, https://doi.org/10.1016/j.applthermaleng.2019.114135.
- [40] Y. Gao, J. Lalevée, A. Simon-Masseron, An overview on 3D printing of structured porous materials and their applications, Adv. Mater. Technol. 8 (2023) 2300377, https://doi.org/10.1002/admt.202300377.
- [41] A. Pereira, A.F.P. Ferreira, A.E. Rodrigues, A.M. Ribeiro, M.J. Regufe, Additive manufacturing for adsorption-related applications—a review, J. Adv. Manuf. Process. 4 (2022) e10108.
- [42] J. Wu, X. Zhu, F. Yang, R. Wang, T. Ge, Shaping techniques of adsorbents and their applications in gas separation: a review, J. Mater. Chem. a. 10 (2022) 22853–22895, https://doi.org/10.1039/D2TA04352A.
- [43] J. Yu, J. Zhu, L. Chen, Y. Chao, W. Zhu, Z. Liu, A review of adsorption materials and their application of 3D printing technology in the separation process, Chem. Eng. J. 475 (2023) 146247, https://doi.org/10.1016/j.cej.2023.146247.
- [44] K. Bharat Jivrakh, S. Kuppireddy, S.E. Taher, K. Polychronopoulou, R. Abu Al-Rub, N. Alamoodi, G.N. Karanikolos, Zeolite-coated 3D-printed gyroid scaffolds for carbon dioxide adsorption, Sep. Purif. Technol. 346 (2024) 127523, https:// doi.org/10.1016/j.seppur.2024.127523.
- [45] S.F. Iftekar, A. Aabid, A. Amir, M. Baig, Advancements and limitations in 3D printing materials and technologies: a critical review, Polymers (Basel) 15 (2023), https://doi.org/10.3390/polym15112519.
- [46] X. Liu, G.J.H. Lim, Y. Wang, L. Zhang, D. Mullangi, Y. Wu, D. Zhao, J. Ding, A. K. Cheetham, J. Wang, Binder-free 3D printing of covalent organic framework

- (COF) monoliths for CO2 adsorption, Chem. Eng. J. 403 (2021) 126333, https://doi.org/10.1016/j.cej.2020.126333.
- [47] S. Royuela, S. Sevim, G. Hernanz, D. Rodríguez-San-Miguel, P. Fischer, C. Franco, S. Pané, J. Puigmartí-Luis, F. Zamora, 3D printing of covalent organic frameworks: a microfluidic-based system to manufacture binder-free macroscopic monoliths, Adv. Funct. Mater. 34 (2024) 2314634, https://doi.org/10.1002/adfm.202314634
- [48] S. Krishnamurthy, R. Roelant, R. Blom, B. Arstad, Z. Li, M. Rombouts, V. Middelkoop, A.B. Borras, L. Naldoni, Scaling up 3D printed hybrid sorbents towards (cost) effective post-combustion CO2 capture: a multiscale study, Int. J. Greenh. Gas Control. 132 (2024) 104069, https://doi.org/10.1016/j. iigec.2024.104069.
- [49] ExxonMobil, QuestAir, Rapid Cycle Pressure Swing Adsorption (RCPSA), (n.d.). https://d3pcsg2wjq9izr.cloudfront.net/files/37735/download/450666/e\_h2x\_62 00\_brochure.pdf.
- [50] Global Thermostat, A uniquely efficient and powerful direct air capture solution, (n.d.). https://www.globalthermostat.com/solutions.
- [51] Climeworks, Direct air capture: our technology to capture CO<sub>2</sub>, (n.d.). htt ps://climeworks.com/direct-air-capture.
- [52] Svante, A New Era of Carbon Capture & Removal Has Arrived, 2023. https://svanteinc.com/carbon-capture-technology/.
- [53] O. Ghaffari-Nik, L. Mariac, A. Liu, B. Henkel, S. Marx, P. Hovington, Rapid Cycle Temperature Swing Adsorption Process Using Solid Structured Sorbent for CO2 capture from Cement Flue Gas, in: Proc. 16th Greenh. Gas Control Technol. Conf., 2022. doi: https://doi.org/10.2139/ssrn.3814414.
- [54] NRG Energy Inc., NRG CO2NCEPT Confirmation of Novel Cost-Effective Emerging Post-Combustion Technology, 2016. https://www.netl.doe.gov/sites/default/files/2017-12/fe0026581-final-report.pdf.
- [55] S. Bale, M. Sathe, O. Ayeni, A.S. Berrouk, J. Joshi, K. Nandakumar, Spatially resolved mass transfer coefficient for moderate Reynolds number flows in packed beds: Wall effects, Int. J. Heat Mass Transf. 110 (2017) 406–415, https://doi.org/ 10.1016/j.ijheatmasstransfer.2017.03.052.
- [56] V. Middelkoop, K. Coenen, J. Schalck, M. Van Sint Annaland, F. Gallucci, 3D printed versus spherical adsorbents for gas sweetening, Chem. Eng. J. 357 (2019) 309–319, https://doi.org/10.1016/j.cej.2018.09.130.
- [57] F.A. Hasan, P. Xiao, R.K. Singh, P.A. Webley, Zeolite monoliths with hierarchical designed pore network structure: Synthesis and performance, Chem. Eng. J. 223 (2013) 48–58, https://doi.org/10.1016/j.cej.2013.02.100.
- [58] S. Krishnamurthy, Vacuum swing adsorption process for post-combustion carbon capture with 3D printed sorbents: quantifying the improvement in productivity and specific energy over a packed bed system through process simulation and optimization, Chem. Eng. Sci. 253 (2022) 117585, https://doi.org/10.1016/j. crs. 2022.117585
- [59] S.N. Sluijter, J. Boon, J. James, S. Krishnamurthy, A. Lind, R. Blom, K. A. Andreassen, A.M. Cormos, V.C. Sandu, R. de Boer, 3D-printing of adsorbents for increased productivity in carbon capture applications (3D-CAPS), Int. J. Greenh. Gas Control. 112 (2021) 103512, https://doi.org/10.1016/j.iigec.2021.103512.
- [60] E. Tegeler, Y. Cui, M. Masoudi, A.M. Bahmanpour, T. Colbert, J. Hensel, V. Balakotaiah, A novel contactor for reducing the cost of direct air capture of CO2, Chem. Eng. Sci. 281 (2023) 119107, https://doi.org/10.1016/j. cos/3023.11017
- [61] D.H. Jeong, M.J. Realff, Modular monolith adsorbent systems for CO2 capture and its parameterized optimization, Chem. Eng. Res. Des. 176 (2021) 1–13, https://doi.org/10.1016/j.cherd.2021.09.018.
- [62] B.G. Keefer, C. Alain, S. Brian, I. Shaw, L. Belinda, Adsorbent laminate structures, US6692626B2, 2002. https://patents.google.com/patent/US6692626B2/en.
- [63] D.J. Connor, D.G. Doman, L. Jeziorowski, K. Bowie G., B. Larisch, C. McLean, I. Shaw, Rotary pressure swing adsorption apparatus, US6406523B1, 2002. https://patents.google.com/patent/US6406523B1/en.
- [64] B.G. Keefer, A.A. Carel, B.G. Sellars, I.S.D. Shaw, B.C. Larisch, D.G. Doman, F.K. Lee, A.C. Gibbs, B.H. Hetzler, J.A. Sawada, A.M. Pelman, C.F. Hunter, Adsorbent coating compositions, laminates and adsorber elements, US7902114B2, 2011. https://patents.google.com/patent/US7902114B2/en?q=(~patent% 2FUS6692626B2).
- [65] B.G. Keefer, High frequency pressure swing adsorption, US6176897B1, 2001. https://patents.google.com/patent/US6176897B1/en?oq=US6%2C176%2C897.
- [66] F.C. Patcas, G.I. Garrido, B. Kraushaar-Czarnetzki, CO oxidation over structured carriers: a comparison of ceramic foams, honeycombs and beads, Chem. Eng. Sci. 62 (2007) 3984–3990, https://doi.org/10.1016/j.ces.2007.04.039.
- [67] J.T. Richardson, Y. Peng, D. Remue, Properties of ceramic foam catalyst supports: pressure drop, Appl. Catal. A Gen. 204 (2000) 19–32, https://doi.org/10.1016/ S0926-860X(00)00508-1.
- [68] P.W.A.M. Wenmakers, J. van der Schaaf, B.F.M. Kuster, J.C. Schouten, Comparative modeling study on the performance of solid foam as a structured catalyst support in multiphase reactors, Ind. Eng. Chem. Res. 49 (2010) 5353–5366, https://doi.org/10.1021/ie900644e.
- [69] E.S. Hevorkian, V.P. Nerubatskyi, R.V. Vovk, T. Szumiata, J.N. Latosińska, Foamy ceramic filters and new possibilities of their applications, Ceram. Int. 50 (2024) 6961–6968, https://doi.org/10.1016/j.ceramint.2023.12.046.
- [70] M. Ambrosetti, M. Bracconi, M. Maestri, G. Groppi, E. Tronconi, Packed foams for the intensification of catalytic processes: assessment of packing efficiency and pressure drop using a combined experimental and numerical approach, Chem. Eng. J. 382 (2020) 122801, https://doi.org/10.1016/j.cej.2019.122801.

- [71] F. Rezaei, P. Webley, Optimum structured adsorbents for gas separation processes, Chem. Eng. Sci. 64 (2009) 5182–5191, https://doi.org/10.1016/j. ces.2009.08.029.
- [72] B. He, J. Liu, Y. Zhang, S. Zhang, P. Wang, H. Xu, Comparison of structured activated carbon and traditional adsorbents for purification of H2, Sep. Purif. Technol. 239 (2020) 116529, https://doi.org/10.1016/j.seppur.2020.116529.
- [73] S. Lawson, B. Adebayo, C. Robinson, Q. Al-Naddaf, A.A. Rownaghi, F. Rezaei, The effects of cell density and intrinsic porosity on structural properties and adsorption kinetics in 3D-printed zeolite monoliths, Chem. Eng. Sci. 218 (2020) 115564, https://doi.org/10.1016/j.ces.2020.115564.
- [74] D.G. Pahinkar, S. Garimella, T.R. Robbins, Feasibility of using adsorbent-coated microchannels for pressure swing adsorption: parametric studies on depressurization, Ind. Eng. Chem. Res. 54 (2015) 10103–10114, https://doi.org/ 10.1021/acs.jecr.5b01023.
- [75] C.Y. Pan, C.W. McMinis, Hollow Fiber Bundle Element, US. Patent No. 5 139 668, 1992.
- [76] X. Feng, C.Y. Pan, C.W. McMinis, J. Ivory, D. Ghosh, Hollow-fiber-based adsorbers for gas separation by pressure-swing adsorption, AIChE J. 44 (1998) 1555–1562. https://doi.org/10.1002/aic.690440709.
- [77] A.R. Sujan, D.-Y. Koh, G. Zhu, V.P. Babu, N. Stephenson, A. Rosinski, H. Du, Y. Luo, W.J. Koros, R.P. Lively, High-temperature activation of zeolite-loaded fiber sorbents, Ind. Eng. Chem. Res. 57 (2018) 11757–11766, https://doi.org/ 10.1021/acs.iecr.8b02210.
- [78] R.P. Lively, R.R. Chance, B.T. Kelley, H.W. Deckman, J.H. Drese, C.W. Jones, W. J. Koros, Hollow fiber adsorbents for CO2 removal from flue gas, Ind. Eng. Chem. Res. 48 (2009) 7314–7324, https://doi.org/10.1021/ie9005244.
- [79] R.P. Lively, R.R. Chance, J.A. Mysona, V.P. Babu, H.W. Deckman, D.P. Leta, H. Thomann, W.J. Koros, CO2 sorption and desorption performance of thermally cycled hollow fiber sorbents, Int. J. Greenh. Gas Control. 10 (2012) 285–294, https://doi.org/10.1016/j.ijggc.2012.06.019.
- [80] B.R. Pimentel, R.P. Lively, Propylene enrichment via kinetic vacuum pressure swing adsorption using ZIF-8 fiber sorbents, ACS Appl. Mater. Interfaces 10 (2018) 36323–36331, https://doi.org/10.1021/acsami.8b08983.
- [81] B. Ohs, J. Lohaus, D. Marten, R. Hannemann-Tamás, A. Krieger, M. Wessling, Optimized hollow fiber sorbents and pressure swing adsorption process for H2 recovery, Ind. Eng. Chem. Res. 57 (2018) 5093–5105, https://doi.org/10.1021/ acs.jecr.7b05368.
- [82] N. Bessho, Advanced pressure swing adsorption system with fiber sorbents for hydrogen recovery, Georgia Institute of Technology, 2010. http://hdl.handle.net/1853/42822.
- [83] D. Ko, R. Siriwardane, L.T. Biegler, Optimization of a pressure-swing adsorption process using zeolite 13X for CO2 sequestration, Ind. Eng. Chem. Res. 42 (2003) 339–348, https://doi.org/10.1021/ie0204540.
- [84] J. Yang, C.-H. Lee, J.-W. Chang, Separation of hydrogen mixtures by a two-bed pressure swing adsorption process using zeolite 5A, Ind. Eng. Chem. Res. 36 (1997) 2789–2798, https://doi.org/10.1021/ie960728h.
- [85] R.P. Lively, N. Bessho, D.A. Bhandari, Y. Kawajiri, W.J. Koros, Thermally moderated hollow fiber sorbent modules in rapidly cycled pressure swing adsorption mode for hydrogen purification, Int. J. Hydrogen Energy. 37 (2012) 15227–15240, https://doi.org/10.1016/j.ijhydene.2012.07.110.
- [86] T. Sen, Y. Kawajiri, M.J. Realff, Adsorption process intensification through structured packing: a modeling study using zeolite 13X and a mixture of propylene and propane in hollow-fiber and packed beds, Ind. Eng. Chem. Res. 58 (2019) 5750–5767, https://doi.org/10.1021/acs.iecr.8b02189.
- [87] Y.H. Lee, J. Jeong, K. Kim, T. Hyun, A. Jamal, D.-Y. Koh, Microporous materials in scalable shapes: fiber sorbents, Chem. Mater. 32 (2020) 7081–7104, https://doi.org/10.1021/acs.chemmater.0c00183.
- [88] D. Pashchenko, Pressure drop in the thermochemical recuperators filled with the catalysts of various shapes: a combined experimental and numerical investigation, Energy 166 (2019) 462–470, https://doi.org/10.1016/j. energy.2018.10.084.
- [89] K. Gopal Manoharan, V.V. Buwa, Structure-resolved CFD simulations of different catalytic structures in a packed bed, Ind. Eng. Chem. Res. 58 (2019) 22363–22375, https://doi.org/10.1021/acs.iecr.9b03537.
- [90] R. Zhang, Y. Shen, Z. Tang, W. Li, D. Zhang, A review of numerical research on the pressure swing adsorption process, Processes. 10 (2022), https://doi.org/ 10.3390/pr10050812.
- [91] S. Guffanti, C.G. Visconti, J. van Kampen, J. Boon, G. Groppi, Reactor modelling and design for sorption enhanced dimethyl ether synthesis, Chem. Eng. J. 404 (2021) 126573, https://doi.org/10.1016/j.cej.2020.126573.
- [92] J. von Seckendorff, O. Hinrichsen, Review on the structure of random packedbeds, Can. J. Chem. Eng. 99 (2021) S703–S733, https://doi.org/10.1002/ cice.23959.
- [93] W. van Antwerpen, C.G. du Toit, P.G. Rousseau, A review of correlations to model the packing structure and effective thermal conductivity in packed beds of monosized spherical particles, Nucl. Eng. Des. 240 (2010) 1803–1818, https://doi.org/ 10.1016/j.nucengdes.2010.03.009.
- [94] T. Allen, in: Particle Size, Shape and Distribution BT Particle Size Measurement, Springer, Netherlands, Dordrecht, 1990, pp. 124–191, https://doi.org/10.1007/ 978-94-009-0417-0-4.
- [95] C.D. Depcik, A.J. Hausmann, Review and a methodology to investigate the effects of monolithic channel geometry, J. Eng. Gas Turbines Power. 135 (2013), https:// doi.org/10.1115/1.4007848.
- [96] C.G. du Toit, P.J. van Loggerenberg, H.J. Vermaak, An evaluation of selected friction factor correlations and results for the pressure drop through random and

- structured packed beds of uniform spheres, Nucl. Eng. Des. 379 (2021) 111213, https://doi.org/10.1016/j.nucengdes.2021.111213.
- [97] E. Érdim, Ö. Akgiray, İ. Demir, A revisit of pressure drop-flow rate correlations for packed beds of spheres, Powder Technol. 283 (2015) 488–504, https://doi.org/ 10.1016/j.powtec.2015.06.017.
- [98] S. Ergun, Fluid flow through packed columns, Chem. Eng. Prog. 48 (1952) 89.
- [99] P.C. Carman, Fluid flow through a granular bed, Trans. Inst. Chem. Eng. London. 15 (1937) 150–156.
- [100] P.N. Dwivedi, S.N. Upadhyay, Particle-fluid mass transfer in fixed and fluidized beds, Ind. Eng. Chem. Process Des. Dev. 16 (1977) 157–165, https://doi.org/ 10.1021/i260062a001.
- [101] J. von Seckendorff, N. Szesni, R. Fischer, O. Hinrichsen, Experimental characterization of random packed spheres, cylinders and rings, and their influence on pressure drop, Chem. Eng. Sci. 222 (2020) 115644, https://doi.org/ 10.1016/j.ces.2020.115644.
- [102] Z. Guo, Z. Sun, N. Zhang, M. Ding, H. Bian, Z. Meng, Computational study on fluid flow and heat transfer characteristic of hollow structured packed bed, Powder Technol. 344 (2019) 463–474, https://doi.org/10.1016/j.powtec.2018.11.101.
- [103] K.G. Allen, T.W. von Backström, D.G. Kröger, Packed bed pressure drop dependence on particle shape, size distribution, packing arrangement and roughness, Powder Technol. 246 (2013) 590–600, https://doi.org/10.1016/j. powtec.2013.06.022.
- [104] N. Mohammadi, R.T. Sanders, C.E. Holland, A.D. Ebner, J.A. Ritter, Non-experimental methodology for developing pressure drop correlations for structured adsorbents with parallel channels, Adsorption. 29 (2023) 29–43, https://doi.org/10.1007/s10450-023-00374-2.
- [105] J. Chaudhuri, A. Baukelmann, K. Boettcher, P. Ehrhard, Pressure drop in fibrous filters, Eur. J. Mech. - B/fluids. 76 (2019) 115–121, https://doi.org/10.1016/j. euromechflu.2019.01.013.
- [106] J. Kalyanaraman, Y. Fan, R.P. Lively, W.J. Koros, C.W. Jones, M.J. Realff, Y. Kawajiri, Modeling and experimental validation of carbon dioxide sorption on hollow fibers loaded with silica-supported poly(ethylenimine), Chem. Eng. J. 259 (2015) 737–751, https://doi.org/10.1016/j.cej.2014.08.023.
- [107] F. Akhtar, L. Andersson, S. Ogunwumi, N. Hedin, L. Bergström, Structuring adsorbents and catalysts by processing of porous powders, J. Eur. Ceram. Soc. 34 (2014) 1643–1666, https://doi.org/10.1016/j.jeurceramsoc.2014.01.008.
- [108] M.T.Q.S. da Silva, M. do Rocio Cardoso, C.M.P. Veronese, W. Mazer, Tortuosity: a brief review, Mater. Today Proc. 58 (2022) 1344–1349, https://doi.org/10.1016/ j.matpr.2022.02.228.
- [109] A.G. Dixon, Correlations for wall and particle shape effects on fixed bed bulk voidage, Can. J. Chem. Eng. 66 (1988) 705–708, https://doi.org/10.1002/ cice.5450660501.
- [110] F. Benyahia, K.E. O'Neill, Enhanced voidage correlations for packed beds of various particle shapes and sizes, Part. Sci. Technol. 23 (2005) 169–177, https:// doi.org/10.1080/02726350590922242.
- [111] C. Ferroni, F.S. Franchi, M. Ambrosetti, M. Bracconi, G. Groppi, M. Maestri, E. Tronconi, Numerical and experimental investigation of pressure drop in periodic open cellular structures for intensification of catalytic processes, ACS Eng. Au. 2 (2022) 118–133, https://doi.org/10.1021/acsengineeringau.1c00034.
- [112] R.T. Yang, Gas separation by adsorption processes, World Scientific, 1997.
- [113] N. Wakao, T. Funazkri, Effect of fluid dispersion coefficients on particle-to-fluid mass transfer coefficients in packed beds: Correlation of sherwood numbers, Chem. Eng. Sci. 33 (1978) 1375–1384, https://doi.org/10.1016/0009-2509(78)
- [114] G. Groppi, L. Giani, E. Tronconi, Generalized correlation for gas/solid masstransfer coefficients in metallic and ceramic foams, Ind. Eng. Chem. Res. 46 (2007) 3955–3958, https://doi.org/10.1021/ie061330g.
- [115] A. Patton, B.D. Crittenden, S.P. Perera, Use of the linear driving force approximation to guide the design of monolithic adsorbents, Chem. Eng. Res. Des. 82 (2004) 999–1009, https://doi.org/10.1205/0263876041580749.
- [116] D.M. Ruthven, S. Farooq, K.S. Knaebel, Pressure Swing Adsorption, Wiley, 1996 https://books.google.nl/books?id=4uG8EAAAQBAJ.
- [117] E. Glueckauf, Theory of chromatography. Part 10.—Formulæ for diffusion into spheres and their application to chromatography, Trans. Faraday Soc. 51 (1955) 1540–1551, https://doi.org/10.1039/TF9555101540.
- [118] C.H. Liaw, J.S.P. Wang, R.A. Greenkorn, K.C. Chao, Kinetics of fixed-bed adsorption: a new solution, AIChE J. 25 (1979) 376–381, https://doi.org/ 10.1002/aic.690250229.
- [119] S. Narayanan, Laminate zeolite structure prepared using papermaking techniques for carbon dioxide capture: synthesis, characterisation and performance, Monash University, 2017. doi: 10.4225/03/58ae3de736198.
- [120] O. Levenspiel, Chemical reaction engineering, John Wiley & Sons, 1998.
- [121] H.J.K. Shabbani, M.R. Othman, S.K. Al- Janabi, A.R. Barron, Z. Helwani, H2 purification employing pressure swing adsorption process: parametric and bibliometric review, Int. J. Hydrogen Energy. 50 (2024) 674–699, https://doi.org/10.1016/j.ijhydene.2023.11.069.
- [122] F. Rezaei, M. Grahn, Thermal management of structured adsorbents in CO2 capture processes, Ind. Eng. Chem. Res. 51 (2012) 4025–4034, https://doi.org/10.1021/ie201057p.
- [123] C. Dhoke, A. Zaabout, S. Cloete, S. Amini, Review on reactor configurations for adsorption-based CO2 capture, Ind. Eng. Chem. Res. 60 (2021) 3779–3798, https://doi.org/10.1021/acs.iecr.0c04547.
- [124] J.-J. Lee, M.-K. Kim, D.-G. Lee, H. Ahn, M.-J. Kim, C.-H. Lee, Heat-exchange pressure swing adsorption process for hydrogen separation, AIChE J. 54 (2008) 2054–2064, https://doi.org/10.1002/aic.11544.

- [125] H.J.K. Shabbani, I. Khairunnisa Shamsudin, N.N. Dezaini, A.A. Abd, M. R. Othman, Effect of adsorption-desorption on hydrogen purity and recovery in non-adiabatic pressure swing mediated by microporous palm kernel shell adsorbent, Fuel 311 (2022) 122550, https://doi.org/10.1016/j.fuel.2021.122550.
- [126] H.J.K. Shabbani, A.A. Abd, M.M. Hasan, Z. Helwani, J. Kim, M.R. Othman, Effect of thermal dynamics and column geometry of pressure swing adsorption on hydrogen production from natural gas reforming, Gas Sci. Eng. 116 (2023) 205047, https://doi.org/10.1016/j.jgsce.2023.205047.
- [127] L.R.S. Rosseau, J.T.A. Jansen, I. Roghair, M. van Sint Annaland, Favorable trade-off between heat transfer and pressure drop in 3D printed baffled logpile catalyst structures, Chem. Eng. Res. Des. 196 (2023) 214–234, https://doi.org/10.1016/j.cherd.2023.06.046
- [128] J. Kwon, H. Ma, A. Giri, P.E. Hopkins, N.B. Shustova, Z. Tian, Thermal conductivity of covalent-organic frameworks, ACS Nano 17 (2023) 15222–15230, https://doi.org/10.1021/acsnano.3c03518.
- [129] H. Ma, Z. Aamer, Z. Tian, Ultrahigh thermal conductivity in three-dimensional covalent organic frameworks, Mater. Today Phys. 21 (2021) 100536, https://doi. org/10.1016/i.mtphys.2021.100536.
- [130] D. Danaci, P.A. Webley, C. Petit, Guidelines for techno-economic analysis of adsorption processes, Front. Chem. Eng. 2 (2021). https://www.frontiersin. org/articles/10.3389/fceng.2020.602430.
- [131] R. Rota, P.C. Wankat, Intensification of pressure swing adsorption processes, AIChE J. 36 (1990) 1299–1312, https://doi.org/10.1002/aic.690360903.
- [132] J.K. Kim, P.C. Wankat, Scaling and intensification procedures for simulated moving-bed systems, AIChE J. 49 (2003) 2810–2821, https://doi.org/10.1002/ aic.690491114.
- [133] J. Zhang, P.A. Webley, Cycle development and design for CO2 capture from flue gas by vacuum swing adsorption, Environ. Sci. Technol. 42 (2008) 563–569, https://doi.org/10.1021/es0706854.
- [134] A. Ntiamoah, J. Ling, P. Xiao, P.A. Webley, Y. Zhai, CO2 capture by vacuum swing adsorption: role of multiple pressure equalization steps, Adsorption 21 (2015) 509–522, https://doi.org/10.1007/s10450-015-9690-8.
- [135] C.M. Rebello, I.B.R. Nogueira, Optimizing CO2 Capture in Pressure Swing Adsorption Units: A Deep Neural Network Approach with Optimality Evaluation and Operating Maps for Decision-Making, ArXiv Prepr. ArXiv2312.03873. (2023). doi: 10.48550/arXiv.2312.03873.
- [136] Z. Wu, H. Wang, C. He, B. Zhang, T. Xu, Q. Chen, The application of physics-informed machine learning in multiphysics modeling in chemical engineering, Ind. Eng. Chem. Res. 62 (2023) 18178–18204, https://doi.org/10.1021/acs.iecr.3c02383.
- [137] W. Bradley, J. Kim, Z. Kilwein, L. Blakely, M. Eydenberg, J. Jalvin, C. Laird, F. Boukouvala, Perspectives on the integration between first-principles and data-driven modeling, Comput. Chem. Eng. 166 (2022) 107898, https://doi.org/10.1016/j.compchemeng.2022.107898.
- [138] A.M. Schweidtmann, E. Esche, A. Fischer, M. Kloft, J.-U. Repke, S. Sager, A. Mitsos, Machine learning in chemical engineering: a perspective, Chemie Ing. Tech. 93 (2021) 2029–2039, https://doi.org/10.1002/cite.202100083.
- [139] A. Mohammadi, F. Sheikholeslam, Intelligent optimization: Literature review and state-of-the-art algorithms (1965–2022), Eng. Appl. Artif. Intell. 126 (2023) 106959, https://doi.org/10.1016/j.engappai.2023.106959.
- [140] A. Swarnkar, A. Swarnkar, Artificial Intelligence Based Optimization Techniques: A Review BT - Intelligent Computing Techniques for Smart Energy Systems, in: A. Kalam, K.R. Niazi, A. Soni, S.A. Siddiqui, A. Mundra (Eds.), Springer Singapore, Singapore, 2020, pp. 95–103.
- [141] M.G.M. Abdolrasol, S.M.S. Hussain, T.S. Ustun, M.R. Sarker, M.A. Hannan, R. Mohamed, J.A. Ali, S. Mekhilef, A. Milad, Artificial neural networks based optimization techniques: a review, Electronics 10 (2021), https://doi.org/ 10.3390/electronics10212689.
- [142] L. Tong, P. Bénard, Y. Zong, R. Chahine, K. Liu, J. Xiao, Artificial neural network based optimization of a six-step two-bed pressure swing adsorption system for hydrogen purification, Energy AI. 5 (2021) 100075, https://doi.org/10.1016/j. egyai.2021.100075.
- [143] J. Xiao, C. Li, L. Fang, P. Böwer, M. Wark, P. Bénard, R. Chahine, Machine learning-based optimization for hydrogen purification performance of layered bed pressure swing adsorption, Int. J. Energy Res. 44 (2020) 4475–4492, https://doi.org/10.1002/er.5225.
- [144] S.G. Subraveti, Z. Li, V. Prasad, A. Rajendran, Machine learning-based multiobjective optimization of pressure swing adsorption, Ind. Eng. Chem. Res. 58 (2019) 20412–20422, https://doi.org/10.1021/acs.iecr.9b04173.
- [145] L.M.C. Oliveira, H. Koivisto, I.G.I. Iwakiri, J.M. Loureiro, A.M. Ribeiro, I.B. R. Nogueira, Modelling of a pressure swing adsorption unit by deep learning and artificial Intelligence tools, Chem. Eng. Sci. 224 (2020) 115801, https://doi.org/ 10.1016/j.ces.2020.115801.
- [146] M.A.F. Martins, A.E. Rodrigues, J.M. Loureiro, A.M. Ribeiro, I.B.R. Nogueira, Artificial Intelligence-oriented economic non-linear model predictive control applied to a pressure swing adsorption unit: syngas purification as a case study, Sep. Purif. Technol. 276 (2021) 119333, https://doi.org/10.1016/j. seppur.2021.119333.
- [147] L.E. Andersson, J. Schilling, L. Riboldi, A. Bardow, R. Anantharaman, Bayesian Optimization for techno-economic analysis of pressure swing adsorption processes, in: L. Montastruc, S.B.T.-C.A.C.E. Negny (Eds.), 32 Eur. Symp. Comput. Aided Process Eng., Elsevier, 2022, pp. 1441–1446. doi: 10.1016/B978-0-323-95879-0.50241-1.
- [148] C. Li, T. Yang, H. Luo, L. Tong, P. Bénard, R. Chahine, J. Xiao, Multi-objective optimization of breakthrough times for hydrogen purification through layered

- bed pressure swing adsorption based on genetic algorithm and artificial neural network model, Int. J. Hydrogen Energy. 52 (2024) 390–405, https://doi.org/10.1016/j.ijhydene.2023.08.357.
- [149] A. Streb, M. Mazzotti, Performance limits of neural networks for optimizing an adsorption process for hydrogen purification and CO2 capture, Comput. Chem. Eng. 166 (2022) 107974, https://doi.org/10.1016/j. compchemeng.2022.107974.
- [150] K.N. Pai, V. Prasad, A. Rajendran, Experimentally validated machine learning frameworks for accelerated prediction of cyclic steady state and optimization of pressure swing adsorption processes, Sep. Purif. Technol. 241 (2020) 116651, https://doi.org/10.1016/j.seppur.2020.116651.
- [151] S.H. Kim, H.O.R. Landa, S. Ravutla, M.J. Realff, F. Boukouvala, Data-driven simultaneous process optimization and adsorbent selection for vacuum pressure swing adsorption, Chem. Eng. Res. Des. 188 (2022) 1013–1028, https://doi.org/ 10.1016/j.cherd.2022.10.002.
- [152] A.H. Farmahini, S. Krishnamurthy, D. Friedrich, S. Brandani, L. Sarkisov, Performance-based screening of porous materials for carbon capture, Chem. Rev. 121 (2021) 10666–10741, https://doi.org/10.1021/acs.chemrev.0c01266.
- [153] V. Subramanian Balashankar, A. Rajendran, Process optimization-based screening of zeolites for post-combustion CO2 capture by vacuum swing adsorption, ACS Sustain. Chem. Eng. 7 (2019) 17747–17755, https://doi.org/10.1021/ acssuschemene.9b04124.
- [154] T.D. Burns, K.N. Pai, S.G. Subraveti, S.P. Collins, M. Krykunov, A. Rajendran, T. K. Woo, Prediction of MOF performance in vacuum swing adsorption systems for postcombustion CO2 capture based on integrated molecular simulations, process optimizations, and machine learning models, Environ. Sci. Technol. 54 (2020) 4536–4544, https://doi.org/10.1021/acs.est.9b07407.
- [155] I.B.R. Nogueira, R.O.M. Dias, C.M. Rebello, E.A. Costa, V.V. Santana, A. E. Rodrigues, A. Ferreira, A.M. Ribeiro, A novel nested loop optimization problem based on deep neural networks and feasible operation regions definition for simultaneous material screening and process optimization, Chem. Eng. Res. Des. 180 (2022) 243–253, https://doi.org/10.1016/j.cherd.2022.02.013.
- [156] A. Rajendran, S.G. Subraveti, K.N. Pai, V. Prasad, Z. Li, How can (or why should) process engineering aid the screening and discovery of solid sorbents for CO2 capture? Acc. Chem. Res. 56 (2023) 2354–2365, https://doi.org/10.1021/acs.accounts.3c00335.
- [157] K.N. Pai, V. Prasad, A. Rajendran, Generalized, adsorbent-agnostic, artificial neural network framework for rapid simulation, optimization, and adsorbent

- screening of adsorption processes, Ind. Eng. Chem. Res. 59 (2020) 16730–16740, https://doi.org/10.1021/acs.iecr.0c02339.
- [158] A. Ward, R. Pini, Efficient Bayesian optimization of industrial-scale pressure-vacuum swing adsorption processes for CO2 capture, Ind. Eng. Chem. Res. 61 (2022) 13650–13668, https://doi.org/10.1021/acs.iecr.2c02313.
- [159] S. Cuomo, V.S. Di Cola, F. Giampaolo, G. Rozza, M. Raissi, F. Piccialli, Scientific machine learning through physics-informed neural networks: where we are and what's next, J. Sci. Comput. 92 (2022) 88, https://doi.org/10.1007/s10915-022-01939-z.
- [160] S. Cai, Z. Mao, Z. Wang, M. Yin, G.E. Karniadakis, Physics-informed neural networks (PINNs) for fluid mechanics: a review, Acta Mech. Sin. 37 (2021) 1727–1738, https://doi.org/10.1007/s10409-021-01148-1.
- [161] S. Cai, Z. Wang, S. Wang, P. Perdikaris, G.E. Karniadakis, Physics-informed neural networks for heat transfer problems, J. Heat Transfer. 143 (2021), https://doi. org/10.1115/1.4050542.
- [162] V.V. Santana, M.S. Gama, J.M. Loureiro, A.E. Rodrigues, A.M. Ribeiro, F. W. Tavares, A.G. Barreto, I.B.R. Nogueira, A first approach towards adsorption-oriented physics-informed neural networks: monoclonal antibody adsorption performance on an ion-exchange column as a case study, ChemEngineering. 6 (2022), https://doi.org/10.3390/chemengineering6020021.
- [163] S.-Y. Tang, Y.-H. Yuan, Y.-C. Chen, S.-J. Yao, Y. Wang, D.-Q. Lin, Physics-informed neural networks to solve lumped kinetic model for chromatography process, J. Chromatogr. A 1708 (2023) 464346, https://doi.org/10.1016/j.chroma.2023.464346.
- [164] S.G. Subraveti, Z. Li, V. Prasad, A. Rajendran, Can a computer "learn" nonlinear chromatography?: Experimental validation of physics-based deep neural networks for the simulation of chromatographic processes, Ind. Eng. Chem. Res. 62 (2023) 5929–5944, https://doi.org/10.1021/acs.iecr.2c04355.
- [165] K.T. Leperi, D. Yancy-Caballero, R.Q. Snurr, F. You, 110th Anniversary: surrogate models based on artificial neural networks to simulate and optimize pressure swing adsorption Cccles for CO2 capture, Ind. Eng. Chem. Res. 58 (2019) 18241–18252, https://doi.org/10.1021/acs.iecr.9b02383.
- [166] N.D. Vo, D.H. Oh, J.-H. Kang, M. Oh, C.-H. Lee, Dynamic-model-based artificial neural network for H2 recovery and CO2 capture from hydrogen tail gas, Appl. Energy. 273 (2020) 115263, https://doi.org/10.1016/j.apenergy.2020.115263.
- [167] S.V. Sivakumar, D.P. Rao, Adsorptive separation of gas mixtures: Mechanistic view, sharp separation and process intensification, Chem. Eng. Process. Process Intensif. 53 (2012) 31–52, https://doi.org/10.1016/j.cep.2011.12.012.